

Automated Design of Macrocycles for Therapeutic Applications: from Small Molecules to Peptides and Proteins

Dan Sindhikara^{1,§,*}, Michael Wagner², Paraskevi Gkeka³, Stefan Güssregen², Garima Tiwari²,
Gerhard Hessler², Engin Yapici¹, Ziyu Li², Andreas Evers^{2,§,*}

¹Schrodinger, Inc., 120 West 45th Street, New York, New York 10036, United States.

²Sanofi-Aventis Deutschland GmbH, Industriepark Hoechst, Frankfurt am Main, Germany.

³Structure Design and Informatics, Sanofi R&D, Chilly-Mazarin, France.

*Correspondence to: Dan Sindhikara, phone: +1 212 548 2371, E-mail:

Dan.Sindhikara@schrodinger.com; Andreas Evers, phone: +49 305 12636, E-mail:

Andreas.Evers@sanofi.com;

Keywords: cyclic peptide(s), macrocycles, stapling, molecular design, molecular modeling, PROTAC, protein-protein interactions

Abstract

Macrocycles and cyclic peptides are increasingly attractive therapeutic modalities as they often have improved affinity, are able to bind to extended protein interfaces and otherwise have favorable properties. Macrocyclization of a known binder molecule has the potential to stabilize its bioactive conformation, improve its metabolic stability, cell permeability and in certain cases oral bioavailability. Herein, we present an *in silico* approach that automatically generates, evaluates and proposes cyclizations utilizing a library of well-established chemical reactions and reagents. Using the three-dimensional (3D) conformation of the linear molecule in complex with a target protein as starting point, this approach identifies attachment points, generates linkers, evaluates the conformational landscape of suitable linkers and their geometric compatibility and ranks the resulting molecules with respect to their predicted conformational stability and interactions with the target protein. As we show here with several prospective and retrospective case studies, this procedure can be applied for the macrocyclization of small molecules and peptides and even PROTACs and proteins. The presented approach is an important step towards the enhanced utilization of macrocycles and cyclic peptides as attractive therapeutic modalities.

(Abstract graphic)

Introduction

During the past decade, macrocycles, defined as cyclic small molecules or peptides typically with a molecular weight of 500 to 2000 Da, have gained significant interest as therapeutic agents, due to the introduction of new approaches for their synthesis and screening.¹⁻³ Moreover, there is an unmet need for therapeutic agents that will be able to target a not yet well addressed type of disease-relevant surfaces and interfaces that include, among others, extra- and intracellular protein-protein interactions (PPIs) with large and shallow (featureless) binding sites typically less amenable to small-molecule drugs.⁴ Because of their size and complexity, macrocycles have demonstrated that they can bind with antibody-like affinity and specificity and successfully target PPIs.⁵⁻¹⁸ Hence, macrocyclic molecules fill an important gap in the world of drugs between small molecules and larger biologics.^{19,20}

Significant progress has been made for peptides in terms of synthesis, formulation and delivery,²¹ but their therapeutic value is partially limited due to their short *in vivo* half-life and lack of oral bioavailability. Moreover, while in solution, peptides span a large conformational space that increases the entropic cost of binding. Cyclization is one of the ways to limit this entropic cost of binding and thus improve its potency. Importantly, it has been shown that constraining a peptide via cyclization can also result in improved selectivity.²²⁻²⁴ Furthermore, cyclization is known to enhance the folding of peptides into conformations that might allow the formation of intramolecular hydrogen bonds, which in turn could improve passive permeability by reducing polar surface area. In addition, cyclization generally reduces degradation in the gut, blood, and tissues by shielding residues from metabolic proteases. Finally, covalent cyclization often enhances stability against thermal and chemical stress (e.g., caused by elevated temperature or presence of denaturants), which is often an important goal in engineering studies for peptides or proteins/enzymes for biotherapeutic or biotechnological applications.²⁵

Medicinal chemistry allows further optimization of cyclic peptides towards drug-likeness and enables the access to the world of non-peptidic macrocycles in drug discovery. Thereby, despite violating some or all of the “Rule of Five” (Ro5) parameters, some naturally occurring, as well as synthetic, peptidic and non-peptidic macrocycles have demonstrated the ability for cell permeability

and oral bioavailability.^{26–34} Indeed, a number of macrocycles with a molecular weight (MW) ranging from 500 to 1500 Da have become successful drugs, with multiple examples that can be administered orally.^{7,35–37}

Meanwhile, a variety of chemical approaches for the cyclization of peptides and small molecules have been described in literature (see reviews^{3,6,29,38–43}). One of the most popular strategies for cyclization is *lactamization*. The first studies on intramolecular amide-bond formation via side-chain stapling were reported by Felix *et al.* for helix stabilization between *i*, *i*+4 spaced amino acids.⁴⁴ Since then, this approach has been further elaborated by many others, exploring linkages with different chain lengths and positioning, as described in detail in a number of reviews^{39,45} and references therein. The formation of carbon-carbon bonds may be facilitated using a *ring-closing metathesis* (RCM) reaction.^{46–48} This approach has been successfully applied to several peptides binding to different biological targets.^{49–55} Another strategy is the Cu(I)-catalyzed azide–alkyne cycloaddition^{56,57} as a prototype of the popular “Click reaction”,⁵⁸ which has been reported by Chorev *et al.* for an analogue of the parathyroid hormone-related peptide^{59,60} and by Wang *et al.* for B-cell CLL/lymphoma 9 (BCL9) α -helical peptides.⁶¹ An alternative approach, photoinduced 1,3-dipolar cycloaddition, the UV-induced reaction between tetrazoles and alkenes, has been applied by Madden *et al.* to staple dual peptide inhibitors of the p53-Mdm2/Mdmx interactions.⁶² Staples may also be introduced with *thioethers* by linking of two cysteines via thiol-ene/-yne reactions^{63–66}, or cysteine arylation and alkylation.^{67–73} Cysteine alkylation with reagents, containing three thiol-reactive groups, can also be used for synthesis of bicyclic structures, when the precursor peptide carries three cysteines.^{74,75} These approaches have been used together with combinatorial chemistry or phage display to screen structurally diverse monocyclic^{76–78} or bicyclic peptides.^{79–81} Recently, it was demonstrated that this chemistry can also be applied to the *in situ* cyclization of proteins.^{82–84} For two proteins, *Staphylococcus aureus* sortase A (SrtA) and the KIX domain from the human CREB binding protein, cysteine residues were introduced in three surface-exposed positions and incubated with a triselectrophilic crosslinker to generate bicyclic enzymes with high tolerance towards thermal and chemical stress.⁸⁴

Given the three-dimensional (3D) structure of a linear peptidic or non-peptidic molecule as starting point, the first goal of cyclization is to maintain the conformation of the bioactive region that is relevant for biological recognition and affinity, and introduce linkers where interactions are either not affected or even further improved. Several studies investigated the optimal positioning and linker lengths for the stabilization of α -helical structures.^{46,59,61,68,85-91} However, peptide-protein recognition is frequently mediated via non-helical structures, such as loops, turns or β -sheets⁹² and might therefore require specific optimization of the linker and its positioning in the linear molecule for conformational stabilization. Considering each residue in a peptide as potential cyclization site and taking into account the diversity of chemical strategies for cyclization might lead to a vast number of molecules that could be synthesized. Implementation of reliable *in silico* approaches for an accurate design are therefore needed to guide experimental efforts towards the most promising compounds.^{82,93-96} To perform rational design, a reliable description of macrocycles' conformational landscape is essential. Unfortunately, the rugged conformational landscape limits the effectiveness of standard approaches for small molecules to reliably predict macrocycle conformations.^{10,97,98} Consequently, significant work has been put into enhanced sampling algorithms towards macrocycle conformation prediction.⁹⁷⁻¹⁰⁹ Additional work has been put into docking or otherwise calculating macrocycle binding free energies.¹¹⁰⁻¹¹⁶ More recently, a structure-based design of peptide macrocycles targeting the interaction site of human adaptor protein 14-3-3 using Free Energy Perturbation (FEP) calculations was proposed.¹¹⁷ In this study, the authors used a small library of truncated derivatives with altered substitution pattern based on a previously reported macrocyclic ligand as starting point and performed FEP combined with replica exchange with solute tempering (REST) molecular dynamics (MD) simulations. Interestingly, the ΔpK_d -values calculated through FEP broadly agree with the experimental trends, while the REST MD simulations provided insights into the origins of affinity differences. Despite the above-mentioned efforts, to the best of our knowledge, there is no computational method available that combines automatic enumeration, evaluation and ranking of the macrocyclizations based on a list of chemical linkers and the 3D structure of a linear reference.

The aim of the present study is the implementation of an approach, which, based on a given ligand structure (ideally in complex with a receptor), will provide *in silico* designed macrocyclic small molecules, peptides or proteins targeting a receptor-ligand or protein-protein interface (antagonists or agonists). The presented approach automatically generates proposals for synthesis by enumerating and screening cyclizations. The screening is based on geometric constraints, conformational rigidity and optionally the predicted interactions of the macrocycles to a target protein. The enumeration uses linkers or breeding structures for cyclization that can be synthesized with well-established chemical reactions utilizing (commercially) available chemical reagents. This list of chemical linkers can be modified by the user to consider specific cyclization chemistries and reagents.

Results and Discussion

Here, we present an overview of the general workflow for the recognition and evaluation of sites for macrocyclization, the identification of compatible chemical linkers and their conformational and enthalpic scoring. To demonstrate the scope of this approach, prospective and retrospective applications for peptides, small molecules and proteins will be shown.

General workflow

Our strategy involves several integrated steps summarized in Figure 1. For technical details, see Experimental section. Briefly, we start with the 3D structure of the linear ligand in complex with the target protein and the premise that this system could benefit from structural stabilization by macrocyclization. Further, expertise in the system and synthetic capabilities may suggest a set of cyclization linkers or breeding groups to construct the linkers and attachment points (“limbs”). With these as inputs along with the complexed linear ligand structure, the approach will generate a full conformational ensemble of linkers, permute pairs of attachment points within the rigid ligand and then geometrically filter limb-pair-linker combinations to eliminate highly strained or otherwise unfavorable ones. The output are 3D structures of complexed cyclized ligands. Additional scoring can reduce the number of synthesis proposals. Since the goal of cyclization is often stabilization of the bioactive conformation, here we run conformational sampling and rank the cyclized ligands according to their calculated conformational propensity. Conformational scoring for small molecules and small peptides is performed using Prime Macrocycle Conformational Sampling (Prime-MCS)^{106,107} and for larger peptides and proteins with MD simulations. An “enthalpic” scoring of the protein-ligand complex can be done using either the empirical scoring function GlideScore^{118,119} or the molecular mechanics-generalized Born surface area (MM/GBSA) method.^{120,121} Rigorous free energy calculations, encapsulating both entropic and enthalpic components, may also be applied in many of these cases.^{116,122} Here, indeed for high speed enthalpic screening, we applied GlideScore for small molecule cyclizations and MM/GBSA otherwise.

Identification of attachment points for cyclization

For the identification of attachment points (see Figure 1a), our approach differentiates between the application for peptides/proteins and small molecules. (i) For *peptides*, the default attachment “vectors” for the introduction of cyclizations are typically the C α -C β bonds within the peptide sequence. Hence, this approach allows to consider any (commercially or internally) available α -amino acid with sidechain groups suitably reactive for cyclisation and the resulting design proposals can be synthesized by classical stepwise (solid-phase) peptide synthesis with a subsequent cyclization step. As an additional option, it is possible to consider the C α -H α vector to introduce D-amino acids for cyclization and conformational stabilization. (ii) For *small molecules*, on the other hand, the positioning of the attachment points for cyclization generally depends on the specific synthetic route of the target molecule. Therefore, our approach allows to define the most suited attachment vectors by specifying atomic numbers or a user-defined substructure (defined as SMARTS¹²³) within the starting molecule. With this procedure, it is also possible to introduce “non-standard” cyclizations into a peptide, such as sidechain-to-tail, head-to-sidechain, head-to-tail or other cyclizations.

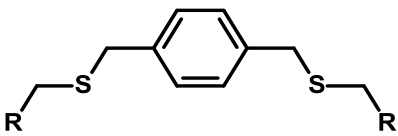
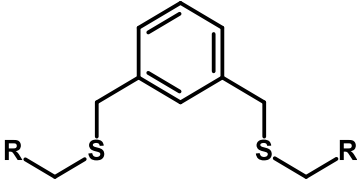
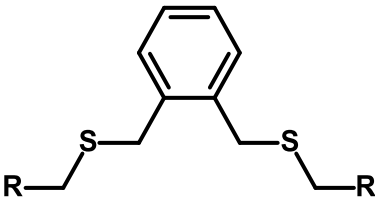
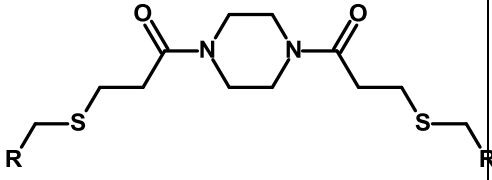
(Figure 1)

Chemical linkers for cyclization

There are two options to obtain chemical linkers for cyclization (see Figure 1b). They can be either (i) provided as explicit list derived from reagents that allow cyclization along a known chemical route or (ii) grown automatically by fusing a set of small spacer fragments. Table 1 provides a list of example linkers which are particularly suited for the sidechain cyclization of peptides. These linkers are derived from common modified amino acids that allow for cyclization via lactamization, click chemistry, ring-closing metathesis or cysteine alkylation. With respect to our *in silico* method, these linkers are attached to the C α -C β or C α -H α vectors of the peptide to design cyclizations via L- or D-amino acids. This list can be easily reduced or extended, for example based on other cyclization chemistry and/or the availability of corresponding reagents, to assure the cyclization proposals can be straightforwardly synthesized. Providing an explicit list of linkers might also be used in a small molecule scenario where the synthetic route is already planned to identify the most promising linkers from a list of available chemical reagents.

Alternatively, rather than specifying predefined cyclization linkers, the linkers can be constructed *in silico* from a small set of “breeding fragments” (see Table 2 for example fragments), combined and enumerated to fit within the geometrical constraints of the ligand-receptor complex. As a result, the algorithm will suggest a diverse set of linker chains that not only span the limb-limb distance, but also are synthetically tractable per the breeding fragment library. While the default spacers shown in Table 2 are amide, PEG, or alkyl moieties, this list of fragments can be expanded, for example to include aromatic rings, heterocycles or other reactive groups.

Table 1. Exemplary chemical linkers for peptide cyclization. Two-armed linkers for the generation of monocycles based on common chemical reagents applying cysteine alkylation, lactamization, ring-closing metathesis or click chemistry. This list can be modified by the user based on specific reagents and chemical cyclization routes.

No	chemistry	structure
1a	cysteine alkylation	
1b	cysteine alkylation	
1c	cysteine alkylation	
1d	cysteine alkylation	

1e	cysteine alkylation	
1f	lactamization	
1g	lactamization	
1h	lactamization	
1i	lactamization	
1j	RCM ^a	
1k	RCM	
1l	RCM	
1m	Click chemistry	
1n	Click chemistry	
1o	Click chemistry	

^aRing-closing Metathesis (RCM)

Table 2. Example breeding fragments for the *in silico* construction and growing of linkers for small molecule cyclization. This list can be modified by the user.

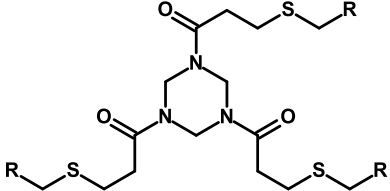
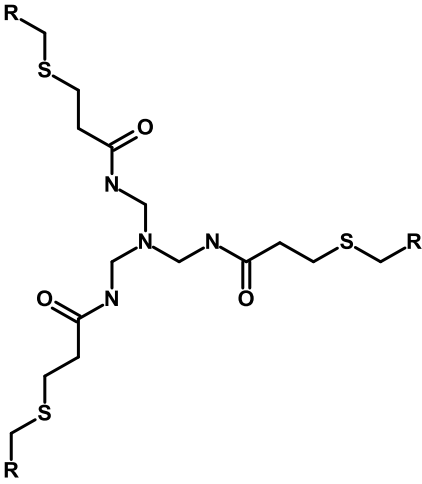
No	name	structure
2a	PEG	
2b	amide	
2c	alkyl	

Generation of bicyclic structures. As mentioned above, it is often advantageous to transform linear peptides or proteins to bicyclic structures, for example via cysteine alkylation using symmetric cyclisation reagents that contain three thiol-reactive groups (see Table 3).^{74,75,79-81} With our approach, it is possible to generate such bicyclic structures in a stepwise fashion as illustrated in Figure 2. First, the tri-symmetrical linker is converted to a two-armed linker with the third limb considered as “non-reactive”. With this two-armed linker, all geometrically reasonable (mono-)cyclized structures are generated as outlined above. In the next step, these cyclized structures are used as the starting points for a second cyclization routine with an appropriate linker, where the previously non-reactive limb is now considered as first attachment point and each C α atom of the peptide backbone as second attachment point.

(Figure 2)

Table 3. Example of three-armed linkers for the generation of bicyclic structures based on common chemical reagents applying cysteine alkylation. This list can be modified by the user.

No	chemistry	structure
3a	cysteine alkylation	

3b	cysteine alkylation	
3c	cysteine alkylation	

Application examples

Peptide example 1: cyclization of dual glucagon-like peptide 1 (GLP-1)/glucagon receptor agonists. We previously described the discovery of dual agonists, which were identified by rational design.^{124,125} Structural elements of glucagon were engineered into the selective GLP-1 receptor agonist exendin-4, resulting in hybrid peptides with potent dual GLP-1/glucagon receptor activity.¹²⁴ Figure 3a shows the predicted binding mode of the dual agonist **4a** in the full-length structure of the GLP-1 receptor. In the first step, we automatically generated cyclization proposals with all chemical linkers shown in Table 1, allowing all residues to be considered as cyclization site. As a result, >2000 linkages were proposed by the cyclization algorithm. Figure 3b illustrates that the algorithm automatically excludes all residues of the linear peptide from cyclization that establish contacts with the GLP-1 receptor, for example in the N-terminal peptide tail where several residues are known to establish interactions that are important for agonistic activity. To reduce the number of synthesis proposals, we next (i) focused on the list of linkers to **1b**, **1f** and **1k** (see Table 1) for cyclization via cysteine alkylation, lactamization or ring-closing metathesis and, (ii) based on SAR knowledge, specified residues 10, 12, 14, 16, 18, 20, 21, 28, 33, 35 and 39 as possible attachment sites for cyclization. With these parameters, 29 cyclization proposals were obtained (see Figure 3c). These proposals were subjected to molecular mechanical minimization and MM/GBSA binding energy calculations with the Prime software (see minimized poses in Figure 3d).¹²⁶ Using the linear peptides **4a** or **4g**, which carry a D-serine (dSer) residue in position 2 for stabilization against DPP IV-mediated cleavage, as structural references, we synthesized ten stapled peptides. Their potency was tested on the GLP-1 and glucagon receptors in a cAMP assay in receptor overexpressing HEK-293 cells (see computed scores and experimental potency data in Table 4).

(Figure 3)

Several *i, i+4* staples were identified along the peptide helix, as in peptides **4b-d** and **4h-i**. Such staples, obtained by lactamization or RCM, have been described for other GLP-1 receptor agonists before¹²⁷⁻¹³⁰ and resulted in improved potency versus the linear reference, presumably by conformational stabilization and/or establishment of additional interactions with the GLP-1 receptor.

Interestingly the potency improvement is not always proportional at the glucagon receptor, presumably due to geometric differences in the receptor structures. These results demonstrate that in addition to potency optimization, cyclization can also be useful to modulate receptor selectivity. In addition to the classical *i, i+4* staples, our algorithm proposed cyclizations within the non-helical peptide region (residues 28-39) that have not been described before: Cyclization via lactamization from position 28 to 33 (peptides **4j** and **4k**) or cysteine alkylation via a meta-xylyl linker (peptide **4e**) maintained or even improved activity at both, the GLP-1 and glucagon receptor.

Based on these findings, we also applied our algorithm for the identification of bicyclic structures (see above) using the three-armed linker **3a** as analog of the two-armed linker **1b**. Due to the geometric constraints of the peptide's 3D structure, only one proposal was obtained (peptide **4f**), which was synthesized using 1,3,5-tris(bromomethyl)benzene (TBMB) as cysteine cross-linker, with Cys residues introduced into positions 21, 28 and 35. EC₅₀ determination revealed, however, a significant drop in potency (> factor 10 at both receptors), which might be attributed to the low conformational score that was obtained from a 100ns MD simulation (see Table 4b). Obviously, the bicycle forces the peptide backbone too far away from the bioactive conformation.

In summary, this prospective case study illustrates that our approach identifies classical motifs for the stabilization of α -helices, but in addition is able to identify favorable cyclizations within non-canonical peptide regions based on the 3D-structure of the reference peptide. These results also demonstrate that the generation of bicyclic structures is technically feasible and that the conformational and enthalpic scores are meaningful measures to prioritize molecules for chemical synthesis.

Table 4. Sequences, computed properties and EC₅₀ Values (plus SEM Values; n=2; measured in pM in a cAMP Assay in overexpressing HEK-293 Cell Lines) of stapled peptidic dual GLP-1/glucagon agonists and their linear references. IUPAC names of all molecules are provided in Table S2.

a)

No	Sequence
4a	HSQGTFTSDLKQMDSRRAQDFIEWLKNGGPSSGAPPPS-NH ₂

b)

No	Sequence modification vs 4a	computed properties		EC ₅₀ [pM] (\pm SEM, n=2)	
		conformational score ^a	enthalpic score ^b	GLP-1R	GCGR
4a		1.69	-193.1	18.3 \pm 1.0	28.6 \pm 1.2
4b	(K10,E14)-lactam	1.44	-187.4	47.5 \pm 3.6	119 \pm 5.0
4c	(Pal ^c 10,Pal14)-RCM	1.62	-192.9	7.4 \pm 0.5	2.3 \pm 0.1
4d	(Pal14,Pal18)-RCM	1.66	-186.5	0.4 \pm 0.0	369 \pm 20.5
4e	(C21,C35,mXyl ^d)-Cys-alk	1.51	-207.3	24.9 \pm 1.2	12.9 \pm 0.9
4f	(C21,C28,C35,Mes ^e)-Cys-alk	2.71	-217.9	194 \pm 14.5	578 \pm 32.0
4g	dSer2	1.69	-217.6	75.4 \pm 3.7	122 \pm 5.5
4h	dSer2;(Pal14,Pal18)-RCM	1.66	-210.6	1.2 \pm 0.1	8430 \pm 610
4i	dSer2;(K16,E20)-lactam	1.35	-219.0	6.4 \pm 0.2	7.8 \pm 0.5
4j	dSer2;(E28,K33)-lactam	1.48	-218.4	14.7 \pm 0.8	54.2 \pm 2.8
4k	dSer2;(K28,E33)-lactam	1.40	-247.9	8.13 \pm 0.3	59.6 \pm 3.9

^athe conformational score was calculated as RMSD over the C α residues (see Supplemental Information for details)

^bthe enthalpic score was obtained from Prime MM/GBSA

^cPal = 4-pentenyl-alanine

^dmXyl = meta-xylyl

^eMes = mesitylene

Peptide example 2: hydrocarbon-stapled peptides targeting β -catenin. One example of helix stabilization using ring-closing metathesis was done in Verdine's group by stapling a helical peptide targeting β -catenin by introduction of two α -methyl, α -alkenyl amino acids (4-pentenyl-alanine or 7-octenyl-alanine).¹³¹ Here, two types of staplings of different linker lengths were attempted, $i,i+7$ staples with D-,L- attachments and $i,i+4$ staples with L-,L- attachments. In that study, three staple configurations were designed and tested (see Table 5). Of them, one stapling improved affinity to β -catenin. We applied our method to see whether this result could be reproduced in an automated, computational fashion. The peptidic precursor structure **5** was taken from pdb code 1qz7 (Figure 4a).

The linkers **1k** and **1l** (Table 1) were, according to the staples used by Grossman *et al.*, set as cyclization options, allowing the consideration of D- and L- attachment at each peptide position. The algorithm produced 64 cyclizations (Figure 4b) including the three (**5b-d**) which were synthesized and tested in the original paper. To accurately mimic the synthetic precursors, these three variants were post-processed by adding an α -methyl to the C_{α} atoms. Subsequently, these postprocessed molecules were scored by (i) conformational stability calculations of the bioactive substructure based on 100 ns unrestrained MD simulations in explicit water in absence of the receptor and (ii) molecular mechanical minimization and MM/GBSA binding energy calculations with the Prime software (see minimized poses in Figure 4c). Table 5 shows the results of the scoring alongside experimental affinities, where measured. From the peptides synthesized in the paper, **5d** is correctly predicted as the most potent according to its predicted enthalpic score. For **5b** and **5c**, the enthalpic score is similar to the linear peptide, which is in line with the experimentally determined K_d values (see Table 5).

(Figure 4)

Table 5. Cyclized peptide inhibitors of β -catenin with predicted conformational and enthalpic scores and reported affinities.¹³¹ The method predicts several staplings to be significantly more stable than those tested in the original manuscript.

a)

No	Sequence
5a	ENPESILDEHVQRVM-NH2

b)

No	Sequence modification vs 5a	computed properties		K_d (mM) ¹³¹
		conformational score ^a	enthalpic score ^b	
5a		1.4	-50.8	~5
5b	(dOal ^c 5,Pal12)-RCM	0.74	-45.7	~3
5c	(Pal ^d 9,Pal13)-RCM	0.8	-52.3	~4
5d	(Pal5,Pal9)-RCM	0.71	-66.9	0.060 \pm 0.002

^athe conformational score was calculated as RMSD over the C α residues of the bioactive region (residues 469-480). See Supplemental Information for details.

^bthe enthalpic score was obtained from Prime MM/GBSA.

^cdOal = D-7-octenyl-alanine

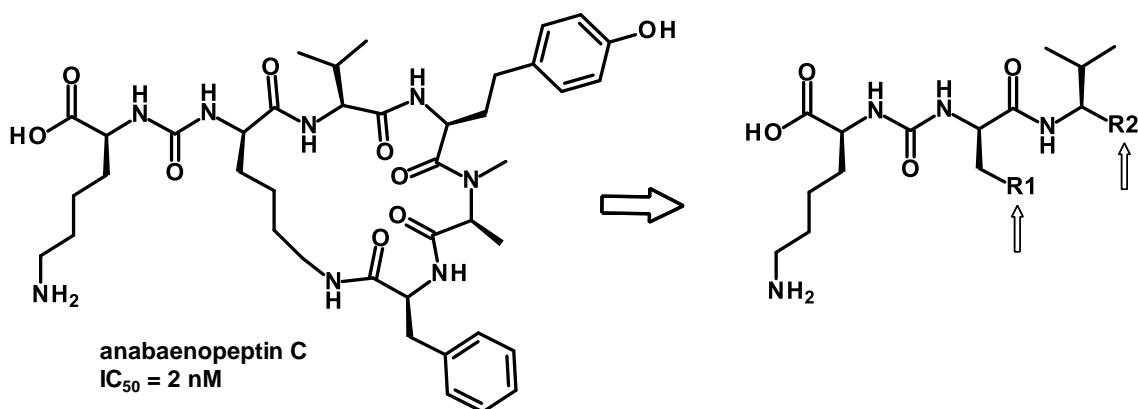
^dPal = 4-pentenyl-alanine

Small molecule example 1: Macrocyclic Inhibitors of Activated Thrombin Activatable Fibrinolysis Inhibitor (TAFIa) from Natural Product Anabaenopeptin. We previously described the identification of anabaenopeptins, cyclic peptides produced by cyanobacteria, as potent inhibitors of TAFIa.¹³² Starting from the x-ray co-crystal structure of anabaenopeptin C bound to the surrogate protease carboxypeptidase B (pdb code 5lrj; see Figure 5a), drug design efforts led to simplified non-cyclic small molecules with increased ligand efficiency.¹³³ In addition, we started a structure-based rational approach towards macrocycles to reduce the size and polar peptidic character of the peptidic ring. Starting from the bioactive conformation of anabaenopeptin C (pdb code 5lrj), we generated a precursor structure with the attachment points for cyclization at the exit vectors of the macrocyclic ring (see Figure 5b and Table 6). To identify suited linkers for cyclization, a set of five “breeding fragments” (see Figure 5c) was provided. Combinatorial enumeration of these fragments would result in >300,000 different linker chains. By automatic consideration of geometrical constraints imposed by the linker attachment vectors and the protein environment, this number was reduced to 68 and further filtered out for unwanted structural motifs, resulting in 45 cyclization proposals. These were docked into the protease binding pocket, ranked according to their enthalpic scores (GlideScore, see Figure 5d) and inspected with respect to their synthetic accessibility. Four macrocyclic analogues were synthesized. IC₅₀ determination (see Table 6) revealed inhibition in the nanomolar range, which is in a similar range compared to other potent small molecule inhibitors of TAFIa that have been reported before.^{133,134}

In conclusion, this prospective study demonstrates how molecules with large peptidic motifs can be converted into lead-like small molecules with favorable ligand efficiency by shrinking and rescaffolding those regions in the peptidic macrocycle that do not establish key interactions with the target protein.

(Figure 5)

Table 6. Macrocyclic derivatives with different linkers and their computed conformational and enthalpic scores. **6a-c** were synthesized and subjected to IC₅₀ determination.



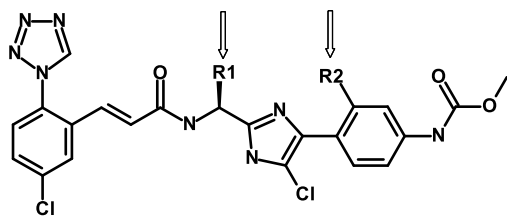
No	linker	computed properties		IC ₅₀ [nM] (±SEM, n=2)
		conformational score ^a	enthalpic score ^b	
6a		1.9	-12.4	52±6
6b		1.5	-12.3	42±3
6c		1.5	-11.7	22±3
6d		1.4	-12.2	10±1

^athe conformational score was calculated by Prime-MCS.

^bthe enthalpic score was obtained from GlideScore.

Small molecule example 2: Macrocyclic Factor XIa Inhibitors. The discovery of novel macrocyclic factor XIa inhibitors based on an acyclic phenyl imidazole lead (Figure 6a) was described in 2017 by Corte *et al* (Bristol-Myers Squibb).¹³⁵ In this publication, several macrocyclic variants of the lead structure have been described that were obtained by structure-based drug design (see selected set of analogues in Table 7). We investigated whether these structures could be designed in an automated fashion with our approach. For this purpose, we generated a precursor structure for cyclization based on the published crystal structure of the acyclic phenyl imidazole lead (pdb code 4y8x, see Figure 6a and b) and provided the linkers shown in Table 7 as input for *in silico* cyclization. In all cases, linker orientations could be found that agree with the geometric constraints imposed by the attachment vectors of the precursor structure (see Figure 6c). For the estimation of conformational stability, a conformational sampling was performed using Prime-MCS (see as example the conformational ensemble of **7e** in Figure 6d). The predicted conformational scores, which were calculated by Prime-MCS, are provided in Table 7. Next, the cyclized ligands were docked with Glide to predict their protein-bound conformations and estimate their enthalpic scores (GlideScore). Notably, the most potent macrocycle **7f** ($K_i = 0.03$ nM), was correctly predicted as (enthalpic) top-scorer. As shown in Figure 6e, the docking modes of all macrocycles are highly similar to the binding orientation of the acyclic lead structure. Figure 6f shows that the predicted binding mode of the macrocyclic compound **7e** is nearly identical to the x-ray structure of a very close analog (pdb code 5tku). In summary, this case study illustrates that our macrocyclization approach can (i) find small molecule macrocyclizations that maintain and stabilize the bioactive conformation of a noncyclic precursor ligand and (ii) identify the most potent analogues by conformational and enthalpic scoring.

Table 7. Macrocyclic derivatives prepared by RCM,¹³⁵ their computed conformational and enthalpic scores and their experimentally measured K_d values.¹³⁵ The linkers shown in this table have been provided as input for the cyclization approach.



No	linker	computed properties		FXIa K _i [nM] ¹³⁵
		conformational score ^a	enthalpic score ^b	
7a		2.7	-11.4	42
7b		2.3	-13.7	250
7c		2.4	-10.4	68
7d		2.9	-12.1	76
7e		2.3	-13.7	0.47
7f		2.6	-14.8	0.03

^athe conformational score was calculated by Prime-MCS.

^bthe enthalpic score was obtained from GlideScore.

(Figure 6)

Cyclization of a PROTAC. PROteolysis TArgeting Chimeras (PROTACs) have become an appealing technology for modulating a protein of interest by degradation.¹³⁶ PROTACs are bifunctional molecules where one ligand binds a protein of interest and the other one an ubiquitin ligase (E3). Both ligands are connected with an optimal linker. Degradation is initiated when PROTACs bind the protein of interest and E3 to form a ternary complex. Recently, Testa *et al.* demonstrated that macrocyclization can also be introduced into PROTACs.¹³⁷ A crystal structure of PROTAC MZ1 (**8a**) in complex with the E3 ligase VHL and its target, the second bromodomain (BD2) of the bromodomain and extra-terminal motif (BET) protein (see Figure 7a), was used as starting point for macrocyclization by introducing a PEG linker at attachment sites that are pointing away from both

proteins (Figure 7b). Despite a loss of binding affinity for BET family member bromodomain-containing protein 4 (Brd4), the macro-PROTAC **8b**, comprising three PEG units, exhibited cellular activity comparable to the linear PROTAC **8a**. Here, we investigated whether this cyclization can be reproduced with our automated approach, using the precursor structure shown in Figure 7b as starting point. For the *in silico* construction and growing of linkers, the PEG fragment **2a** (Table 2) was provided as breeding fragment. This fragment was combined and enumerated to fit within the geometrical constraints of the ligand-protein binding sites. Six linkers comprising 3 to 8 PEG units were identified, including the 3-PEG linker, which was synthesized (**8b**) and successfully tested by Testa *et al.* All macrocyclic PROTAC proposals were subjected to MM/GBSA binding energy calculations with the Prime software (see minimized poses in Figure 7c). Comparison of **8b** with the x-ray structure (pdb code 6sis) reveals that that the experimental binding pose could be well reproduced (see Figure 7d).

Due to their high molecular weight, a major optimization parameter of PROTACs is often their cellular activity.^{136,138} This case study demonstrates the applicability of our *in silico* macrocyclization approach for PROTACs and might therefore represent an interesting strategy to enhance their drug likeness by improving cell permeability and cellular stability.

(Figure 7)

Protein example: generation of bicyclic structures of the KIX domain from the human CREB binding protein for thermal stabilization. The KIX domain (kinase-inducible domain (KID) interaction domain) is an adaptor domain of transcriptional co-activator CREB (cAMP response element-binding) protein with two different protein binding partners and is composed of a central three α -helix bundle ($\alpha 1$, $\alpha 2$, $\alpha 3$). The junction between this bundle and the C-terminal 3_{10} helix (G_1) is crucial for structural integrity (Figure 8a).¹³⁹ Recently, Pelay-Gimeno *at al.* presented an *in situ* protein stabilization procedure (INCYPRO) that involves the introduction of three surface-exposed cysteine residues placed at different secondary structure elements while still being in spatial proximity.⁸⁴ The recombinantly produced construct with cysteine residues in three different positions is then reacted with a triselectrophile for covalent cyclization. With this approach, a bicyclic variant of the KIX

domain was designed that was cyclized via positions 594, 599 and 646 and exhibited strongly increased thermal stability while still showing functional binding activity.

In this case study, we investigated whether our *in silico* cyclization approach is able to automatically generate this bicyclic construct. In analogy to the procedure described by Pelay-Gimeno *et al.*, residues around the C-terminal G₁ helix were selected as attachment sites for the generation of trivalently-linked structures (see Figure 8a) using linker **3c** (Table 3). Applying our procedure for the automatic generation of bicyclic structures (see above), 122 proposals were obtained including the construct designed by Pelay-Gimeno *et al.* Both, the cyclized construct and the natural protein were subjected to a 100 ns unrestrained MD simulation at elevated temperature (340 K) in explicit water in order to rationalize the experimentally observed improvement of the cyclized variant in thermal stability. Whereas the conformational fluctuation in the lower unconstrained region of the helix bundle is similar between the cyclized and non-cyclized variant (see Figures 8c and d), the region where helix G₁ is covalently linked to α_1 and α_2 is – in agreement with the improved thermal stability data reported by Pelay-Gimeno *et al.* - conformationally more stable (RMSD_{C α} 1.04 Å vs 1.72 Å).

This case demonstrates the applicability of *in silico* cyclization as suitable method for the engineering of proteins for increased tolerance towards thermal and chemical denaturation.⁸⁴

(Figure 8)

Summary and Conclusion

Peptidic and non-peptidic macrocycles represent an underexplored class of drugs with properties that could address current deficiencies of peptide and small-molecule drugs.⁹⁶ Therefore, cyclization of molecules from small molecules to peptides and proteins is an important approach in pharmaceutical design. Here, we've designed, implemented, and applied a computational algorithm to automatically generate cyclized molecules and screen them using conformational and enthalpic scoring. This approach can be applied to different modalities and consider peptidic and non-peptidic structural motifs. Through numerous case studies on both retrospective and prospective data, we've shown that the method is able to generate numerous reasonable cyclizations including ones generated from simple breeding units. The method incorporates user-dictated synthetic capabilities and constraints to ensure feasible proposals. Coupled with conformational and enthalpic scoring, the method can suggest cyclizations with favorable binding properties as well. This cyclization and scoring strategy is meanwhile routinely used in early discovery projects at Sanofi. Potential future advances in predicting permeability¹⁴⁰ and pharmacokinetic properties of macrocycles will further strengthen the applicability of the presented method for the multi-parameter optimization of macrocycles. Taken together this approach marks a large step forward in accelerated pharmaceutical design via efficient molecular cyclization.

Experimental section

Algorithmic details of the cyclizer

The cyclization method proceeds from a complexed ligand to a series of cyclized ligands which have been geometrically screened. There are two “modes” for the workflow: “small molecule” and “peptide”. Though there are many similarities, some key differences made splitting of the two modes more efficient. Either mode will attempt to construct geometrically stable and chemically reasonable linkers to span the cyclization length in a manner that does not negatively affect the complex structure (e.g. by introducing strain, clashes, or breaking good interactions). For small molecules, there are typically fewer potential attachment points, and a series of “spacers” to span the cyclization length, which can be pieced together to fill the space. For peptides, the attachment points are fixed but numerous (e.g., all sidechains), and the linkers tend to be of fixed length (e.g., known sidechain bridges). Figure 9 show a breakdown of the two modes.

(Figure 9)

For specific cases, it is possible to “mix” the peptide and small molecule approach. In a small molecule scenario, for example, the user can specify an explicit list of linkers (e.g., based on a list of available chemical reagents) that will not be enumerated and pieced together, but will be directly mapped onto the user-specified attachment points of the ligand. For a peptide, on the other hand, it is possible to evaluate other attachment points than the $C\alpha-C\beta$ or $C\alpha-H\alpha$ vector, for example for the introduction of head-to-sidechain, sidechain-to-tail, head-to-tail cyclizations or for a rescaffolding of the backbone of a peptide within a macrocycle.

Detailed description of the workflow

Input. The user must specify a complexed structure for cyclization, and it may be required to identify the ligand (this is sometimes nontrivial for peptide complexes as peptide ligands are chemically similar to proteins). The user must specify a mode, and for the small molecule mode must specify chemical linkers using SMILES patterns, or for the peptide mode must specify sidechain bridges either by name or by SMILES. All these inputs are sanity checked to confirm no obvious problems.

Limb recognition. For peptide cyclizations, typically all sidechain C α -C β and C α -H α vectors are considered as potential limbs. This can be further controlled by specifying a subregion to target using Schrodinger's Atom Selection Language (ASL). This may especially useful if there is a larger peptide system and there is some knowledge of the system that would preclude some regions from cyclization. For small molecules, users specify criteria for identifying potential branch points (such as ASL, SMARTS, or manually selecting limbs for cyclization).

Small molecule linker construction. In order to limit the combinatorics of permuting linkers, a minimum and maximum linker length is calculated using the recognized limbs. Then linkers are enumerated using combinations of the specified spacers that could potentially span the distance within the range. These constructed linkers are then filtered using simple chemical rules to avoid unchemical linkers (e.g. avoid -OO- or -NN- linkages).

Limb pair filtering. All combinations of limb pairs are enumerated and filtered hierarchically to eliminate unphysical constructions. The pairs are filtered if they either have too few bonds between them or too few bonds per distance¹⁴¹ spanned to eliminate inefficient cyclization. Then the linker is conformationally sampled. Subsequently, using the conformations, the remaining limbs are filtered whether they match the limb distance and orientations seen in the conformational ensemble.

Attach linker precursors. For small molecules, the entire constructed linker is attached to one of the limbs. For peptides, each limb sidechain is mutated to either an L- or D- Alanine (according to the specified chirality), then portions of the linker are attached to either sidechain, leaving "dangling" sidechains.

Close linker. The dangling linkers are then closed by slowly bringing the closing bond atoms closer to each other and finally forming the bond. This process can be time consuming as the bond closing often runs into steric or strain issues.

Post minimize and filter. Finally, the system is minimized and strain filters are applied to assure no highly strained linkers have been built. The cyclized molecules are then output for further analysis.

Implementation

The macrocyclization script has been implemented via command-line in Schrodinger software as of release 2020-1. To run use `$$SCHRODINGER/run -FROM psp macrocyclize -h`

Molecular dynamics simulations

MD simulations were carried out using an explicit solvent MD package, Desmond program (version 4.7, Desmond Molecular Dynamics System; D. E. Shaw Research, New York, NY, USA and version 3.1, Maestro-Desmond Interoperability Tools; Schrödinger) with inbuilt optimized potentials for liquid simulation (OPLS 2.1) force field.^{142–144} The proteins were prepared for simulation by first checking their correctness using the Protein Preparation wizard tool and Epik module was used for deriving the protonation states of the proteins at neutral pH. The system was prepared by placing the proteins in a cubic box with periodic boundary conditions specifying the shape and size of box as 10 Å × 10 Å × 10 Å distance. Predefined TIP3P water model was used as a solvent and the systems were neutralized by adding appropriate number of ions. The solvated systems were relaxed by implementing Steepest Descent and the limited-memory Broyden-Fletcher-Goldfarb-Shanno algorithms in a hybrid manner. The simulation was performed under NPT ensemble for 100ns implementing the Berendsen thermostat and barostat methods. Nose-Hoover thermostat algorithm^{145,146} was used to maintain a constant temperature and MartynaTobias-Klein Barostat algorithm¹⁴⁷ was employed for maintaining 1 atm of pressure throughout the simulation, respectively. The short-range coulombic interactions were analyzed using the short-range method with a cut-off value of 9.0 Å. The Particle Mesh Ewald (PME) method¹⁴⁸ was used for treating the long-range electrostatic interactions. All bonds involving hydrogen atoms were constrained using the SHAKE algorithm.¹⁴⁹

Enthalpic scoring

For small molecules, binding poses of cyclized molecules were predicted with Glide using integrating macrocycle ring sampling.¹¹¹ Enthalpic scoring of the protein-ligand complex was done using the empirical scoring function GlideScore^{118,119}. For larger systems, the cyclized molecules were minimized in the protein environment and the molecular mechanics-generalized Born surface area (MM/GBSA) method^{120,121} was used as enthalpic score.

Conformational scoring

Conformational scoring was performed using Schrödinger's macrocycle conformational stability script.¹⁰⁷ Briefly, the script scores compounds on their propensity to maintain the specified bioactive substructure given a sampled ensemble. Here, macrocyclizations of small molecules were scored as described in the paper, using Prime-MCS to generate a conformational ensemble, then using the stability script to estimate the expected RMSD in the bioactive substructure using Boltzmann weighting at 298.13K. For peptide and protein systems, simple NPT MD was run for 100ns. The stability script here does not need to Boltzmann weight since the conformers already obey the NPT distribution. The bioactive substructure was defined uniquely for each system as is recommended and the conformational score is provided as average RMSD over the C α atoms of the bioactive region.

Synthesis of Peptides

Solid phase synthesis was carried out on a typical Rink-resin (e.g. from Agilent Technologies with a loading of 0.38 mmol/g, 75-150 μ m). The Fmoc-synthesis strategy was applied with HBTU/DIPEA-activation. The peptide was cleaved from the resin with King's cocktail.¹⁵⁰ For the synthesis of cyclic lactam containing peptides, orthogonal protecting groups were used (Allyl/Alloc for the cyclization residues). For the synthesis of hydrocarbon stapled peptides via ring closing metathesis (RCM), corresponding amino acids with alkene side chains were used. On resin cyclization was achieved by treatment of the resin with the Hoveyda-Grubbs Second Generation Catalyst from Aldrich. Finally, for the synthesis of cysteine alkylated peptides, cross-linking was achieved by addition of the cross-linker (1,3-bis(bromomethyl)benzene for **4e** and 1,3,5-tris(bromomethyl)benzene for **4f**) to the Cys deprotected peptides. The crude product was purified via preparative HPLC on a Waters column (e.g. XBridge, BEH130, Prep C18, 5 μ M) using an acetonitrile/water gradient (both buffers with 0.1% TFA). Purity and chemical identity of the product were assessed by UPLC and LC-MS (for details see Table S1) and confirmed to have \geq 95% purity for all key compounds.

In vitro cellular assays for GLP-1 and glucagon receptor potency

Agonism of peptides for the two receptors was determined by functional assays measuring cAMP response of HEK-293 cell lines stably expressing human GLP-1 or glucagon receptor. The cells were

grown in a T-175 culture flask placed at 37°C to near confluence in medium (DMEM / 10% FBS) and collected in 2 ml vials in cell culture medium containing 10% DMSO in concentration of 10-50 million cells /ml. Each vial contained 1.8 ml cells. The vials were slowly frozen to -80 °C in isopropanol, and then transferred in liquid nitrogen for storage. Prior to their use, frozen cells were thawed quickly at 37 °C and washed (5 min at 900 rpm) with 20 ml cell buffer (1x HBSS; 20 mM HEPES, plus 0.1% HSA). Cells were resuspended in assay buffer (cell buffer plus 2 mM IBMX) and adjusted to a cell density of 1 million cells/ml. For measurement of cAMP generation, 5 µl cells (final 5000 cells/well) and 5 µl of test compound were added to a 384-well plate, followed by incubation for 30 min at room temperature. The cAMP generated was determined using a kit from Cisbio Corp. based on HTRF (Homogenous Time Resolved Fluorescence). The cAMP assay was performed according to manufacturer's instructions (Cisbio). After addition of HTRF reagents diluted in lysis buffer (kit components), the plates were incubated for 1 h, followed by measurement of the fluorescence ratio at 665 / 620 nm. In vitro potency of agonists was quantified by determining the concentrations that caused 50% activation of the maximal response (EC₅₀). Reported values are mean (±SEM) EC₅₀ (pM) from n = 2 values within a single experiment.

Synthesis of TAFIa inhibitors

All solvents used were commercially available and were used without further purification. Reactions were typically run using anhydrous solvents (unless otherwise noted) under an inert atmosphere of argon. Starting materials used were available from commercial sources. ¹H NMR spectra were recorded in the indicated deuterated solvent at 500 MHz. Purity of all compounds tested in biological assays were determined to be of ≥95% purity by LC-MS. Detailed synthesis procedures and analytical data are provided in the Supplemental Information.

In vitro cellular assays for TAFIa inhibition

The prepared substance was tested for TAFIa inhibition using the Actichrome plasma TAFI Activity Kit from American Diagnostica (Pr. No. 874). This entailed adding 28 µl of assay buffer (20 mM Hepes, 150 mM NaCl, pH 7.4) and 10 µl of TAFIa (American Diagnostica Pr. No. 874TAFIA; 2.5 µg/ml) to 2 µl of 2.5 mM DMSO solution of the substance and incubating in a 96 half-well microtiter

plate at room temperature for 15 minutes. The enzyme reaction was started by adding 10 μ l of TAFIa developer (prediluted 1:2 with assay buffer). The time course of the reaction was followed at 420 nm in a microtiter plate reader (SpectraMax plus 384; Molecular Devices) for 15 minutes. The IC₅₀ value was calculated from the averaged values (duplicate determination) of serial dilutions of the substance with the aid of the Softmax Pro software (version 4.8; Molecular Devices). Reported values are mean (\pm SEM) IC₅₀ from n = 2 values within a single experiment.

Associated content.

Supporting information. Analytical data with RP-HPLC retention times and molecular masses of the synthesized peptides. IUPAC names of synthesized peptides. Detailed synthesis procedures and analytical data for TAFIa inhibitors. Molecular formula strings.

Corresponding Author Information. Dan Sindhikara, phone: +1 212 548 2371, E-mail: Dan.Sindhikara@schrodinger.com. *Andreas Evers: Phone: +49 305 12636. E-mail: Andreas.Evers@sanofi.com.

Abbreviations Used. 3D, 3-dimensional; alk, alkyl; ASL, atom selection language; BCL9, B-cell CLL/lymphoma 9; BD, bromodomain; BET, bromodomain and extraterminal domain; Brd4, bromodomain 4; cAMP, cyclic adenosine monophosphate; CREB, cAMP response element-binding protein; DCM, dichloromethane; DIPEA, N,N-diisopropylethylamine; DMEM, Dulbecco's modified Eagle's medium; DMSO, dimethyl sulfoxide; dOal, D-7-octenyl-alanine; DPP IV, dipeptidyl peptidase IV; E3, E3 ubiquitin ligase; Elo, elongin; FBS, fetal bovine serum; FEP, free energy perturbation; Fmoc, fluorenylmethoxycarbonyl; GLP-1, glucagon-like peptide-1; GLP-1R, glucagon-like peptide-1 receptor; HBSS, Hank's balanced salt solution; HBTU, O-(Benzotriazole-1-yl)-1,1,3,3-tetramethyluronium hexafluorophosphate; HEK, human embryonic kidney; HEPES, 4-(2-hydroxyethyl)-1-piperazineethanesulfonic acid; HPLC, high-performance liquid chromatography; HSA, human serum albumin; HTRF, homogenous time resolved fluorescence; IBMX, isobutylmethylxanthine; LC-MS, liquid chromatography–mass spectrometry; KIX domain, kinase-inducible domain (KID) interacting domain; MD, molecular dynamics; Mes, mesitylene; MM/GBSA, molecular mechanics-generalized Born surface area; MW, molecular weight; mXyl, meta-Xylyl; NMR, nuclear magnetic resonance; PEG, polyethylene glycol; Prime-MCS, Prime macrocycle conformational sampling; PROTACs, proteolysis targeting chimeras; RCM, ring-closing metathesis; REST, replica exchange with solute tempering; Ro5, rule-of-five; RMSD, root-mean-square deviation; RT, room temperature; SAR, structure-activity relationship; SEM, standard error of the mean; SMARTS, SMILES arbitrary target specification; SMILES, simplified molecular-input line-entry system; SrtA, staphylococcus aureus sortase A; TAFI, thrombin activatable fibrinolysis

inhibitor; TBMB, 1,3,5-tris(bromomethyl)benzene; TFA, trifluoroacetic acid; THF, tetrahydrofuran; UPLC, ultra-performance liquid chromatography; UV, ultraviolet; VHL, von Hippel–Lindau protein;

Acknowledgements. We thank R. Loder and R. Dharanipragada for peptide synthesis; H. Köhler and J. Czech for in vitro potency characterization; C. Poeverlein, E. Feyfant, K. Borrelli, T. Day, and J. Knight for helpful discussions.

References

- (1) Dougherty, P. G.; Qian, Z.; Pei, D. Macrocycles as Protein-Protein Interaction Inhibitors. *Biochem. J.* **2017**, *474* (7), 1109–1125. <https://doi.org/10.1042/BCJ20160619>.
- (2) K. Yudin, A. Macrocycles: Lessons from the Distant Past, Recent Developments, and Future Directions. *Chem. Sci.* **2015**, *6* (1), 30–49. <https://doi.org/10.1039/C4SC03089C>.
- (3) Zaretsky, S.; Yudin, A. K. Recent Advances in the Synthesis of Cyclic Pseudopeptides. *Drug Discov. Today Technol.* **2017**, *26*, 3–10. <https://doi.org/10.1016/j.ddtec.2017.11.004>.
- (4) Mabonga, L.; Kappo, A. P. Protein-Protein Interaction Modulators: Advances, Successes and Remaining Challenges. *Biophys. Rev.* **2019**, *11* (4), 559–581. <https://doi.org/10.1007/s12551-019-00570-x>.
- (5) Abdalla, M. A.; McGaw, L. J. Natural Cyclic Peptides as an Attractive Modality for Therapeutics: A Mini Review. *Mol. Basel Switz.* **2018**, *23* (8). <https://doi.org/10.3390/molecules23082080>.
- (6) Ali, A. M.; Atmaj, J.; Van Oosterwijk, N.; Groves, M. R.; Dömling, A. Stapled Peptides Inhibitors: A New Window for Target Drug Discovery. *Comput. Struct. Biotechnol. J.* **2019**, *17*, 263–281. <https://doi.org/10.1016/j.csbj.2019.01.012>.
- (7) Giordanetto, F.; Kihlberg, J. Macrocyclic Drugs and Clinical Candidates: What Can Medicinal Chemists Learn from Their Properties? *J. Med. Chem.* **2014**, *57* (2), 278–295. <https://doi.org/10.1021/jm400887j>.
- (8) Lee, A. C.-L.; Harris, J. L.; Khanna, K. K.; Hong, J.-H. A Comprehensive Review on Current Advances in Peptide Drug Development and Design. *Int. J. Mol. Sci.* **2019**, *20* (10). <https://doi.org/10.3390/ijms20102383>.
- (9) Naylor, M. R.; Bockus, A. T.; Blanco, M.-J.; Lokey, R. S. Cyclic Peptide Natural Products Chart the Frontier of Oral Bioavailability in the Pursuit of Undruggable Targets. *Curr. Opin. Chem. Biol.* **2017**, *38*, 141–147. <https://doi.org/10.1016/j.cbpa.2017.04.012>.
- (10) Poongavanam, V.; Danelius, E.; Peintner, S.; Alcaraz, L.; Caron, G.; Cummings, M. D.; Wlodek, S.; Erdelyi, M.; Hawkins, P. C. D.; Ermondi, G.; Kihlberg, J. Conformational Sampling of Macrocyclic Drugs in Different Environments: Can We Find the Relevant Conformations? *ACS Omega* **2018**, *3* (9), 11742–11757. <https://doi.org/10.1021/acsomega.8b01379>.
- (11) Qian, Z.; Dougherty, P. G.; Pei, D. Targeting Intracellular Protein-Protein Interactions with Cell-Permeable Cyclic Peptides. *Curr. Opin. Chem. Biol.* **2017**, *38*, 80–86. <https://doi.org/10.1016/j.cbpa.2017.03.011>.
- (12) Robertson, N. S.; Spring, D. R. Using Peptidomimetics and Constrained Peptides as Valuable Tools for Inhibiting Protein-Protein Interactions. *Mol. J. Synth. Chem. Nat. Prod. Chem.* **2018**, *23* (4). <https://doi.org/10.3390/molecules23040959>.
- (13) Rubin, S.; Qvit, N. Cyclic Peptides for Protein-Protein Interaction Targets: Applications to Human Disease. *Crit. Rev. Eukaryot. Gene Expr.* **2016**, *26* (3), 199–221. <https://doi.org/10.1615/CritRevEukaryotGeneExpr.2016016525>.
- (14) Russo, A.; Aiello, C.; Grieco, P.; Marasco, D. Targeting “Undruggable” Proteins: Design of Synthetic Cyclopeptides. *Curr. Med. Chem.* **2016**, *23* (8), 748–762. <https://doi.org/10.2174/0929867323666160112122540>.
- (15) Stone, T. A.; Deber, C. M. Therapeutic Design of Peptide Modulators of Protein-Protein Interactions in Membranes. *Biochim. Biophys. Acta Biomembr.* **2017**, *1859* (4), 577–585. <https://doi.org/10.1016/j.bbamem.2016.08.013>.
- (16) Wójcik, P.; Berlicki, Ł. Peptide-Based Inhibitors of Protein-Protein Interactions. *Bioorg. Med. Chem. Lett.* **2016**, *26* (3), 707–713. <https://doi.org/10.1016/j.bmcl.2015.12.084>.
- (17) Yamagishi, Y.; Shoji, I.; Miyagawa, S.; Kawakami, T.; Katoh, T.; Goto, Y.; Suga, H. Natural Product-like Macrocyclic N-Methyl-Peptide Inhibitors against a Ubiquitin Ligase Uncovered from a Ribosome-Expressed de Novo Library. *Chem. Biol.* **2011**, *18* (12), 1562–1570. <https://doi.org/10.1016/j.chembiol.2011.09.013>.
- (18) Zorzi, A.; Deyle, K.; Heinis, C. Cyclic Peptide Therapeutics: Past, Present and Future. *Curr. Opin. Chem. Biol.* **2017**, *38*, 24–29. <https://doi.org/10.1016/j.cbpa.2017.02.006>.

- (19) Ermert, P. Design, Properties and Recent Application of Macrocycles in Medicinal Chemistry. *Chimia* **2017**, *71* (10), 678–702. <https://doi.org/10.2533/chimia.2017.678>.
- (20) Ermert, P.; Luther, A.; Zbinden, P.; Obrecht, D. Frontier Between Cyclic Peptides and Macrocycles. *Methods Mol. Biol. Clifton NJ* **2019**, *2001*, 147–202. https://doi.org/10.1007/978-1-4939-9504-2_9.
- (21) Lau, J. L.; Dunn, M. K. Therapeutic Peptides: Historical Perspectives, Current Development Trends, and Future Directions. *Bioorg. Med. Chem.* **2018**, *26* (10), 2700–2707. <https://doi.org/10.1016/j.bmc.2017.06.052>.
- (22) Hruby, V. J. Peptide Science: Exploring the Use of Chemical Principles and Interdisciplinary Collaboration for Understanding Life Processes. *J. Med. Chem.* **2003**, *46* (20), 4215–4231. <https://doi.org/10.1021/jm0303103>.
- (23) Hruby, V. J. Designing Peptide Receptor Agonists and Antagonists. *Nat. Rev. Drug Discov.* **2002**, *1* (11), 847–858. <https://doi.org/10.1038/nrd939>.
- (24) Kessler, H. Conformation and Biological Activity of Cyclic Peptides. *Angew. Chem. Int. Ed. Engl.* **1982**, *21* (7), 512–523. <https://doi.org/10.1002/anie.198205121>.
- (25) Purkayastha, A.; Kang, T. J. Stabilization of Proteins by Covalent Cyclization. *Biotechnol. Bioprocess Eng.* **2019**, *24* (5), 702–712. <https://doi.org/10.1007/s12257-019-0363-4>.
- (26) Chu, Q.; Moellering, R. E.; Hilinski, G. J.; Kim, Y.-W.; Grossmann, T. N.; Yeh, J. T.-H.; Verdine, G. L. Towards Understanding Cell Penetration by Stapled Peptides. *MedChemComm* **2015**, *6* (1), 111–119. <https://doi.org/10.1039/C4MD00131A>.
- (27) Dougherty, P. G.; Sahni, A.; Pei, D. Understanding Cell Penetration of Cyclic Peptides. *Chem. Rev.* **2019**, *119* (17), 10241–10287. <https://doi.org/10.1021/acs.chemrev.9b00008>.
- (28) Drucker, D. J. Advances in Oral Peptide Therapeutics. *Nat. Rev. Drug Discov.* **2019**. <https://doi.org/10.1038/s41573-019-0053-0>.
- (29) Jing, X.; Jin, K. A Gold Mine for Drug Discovery: Strategies to Develop Cyclic Peptides into Therapies. *Med. Res. Rev.* **2019**. <https://doi.org/10.1002/med.21639>.
- (30) Nielsen, D. S.; Shepherd, N. E.; Xu, W.; Lucke, A. J.; Stoermer, M. J.; Fairlie, D. P. Orally Absorbed Cyclic Peptides. *Chem. Rev.* **2017**, *117* (12), 8094–8128. <https://doi.org/10.1021/acs.chemrev.6b00838>.
- (31) Nielsen, D. S.; Lohman, R.-J.; Hoang, H. N.; Hill, T. A.; Jones, A.; Lucke, A. J.; Fairlie, D. P. Flexibility versus Rigidity for Orally Bioavailable Cyclic Hexapeptides. *Chembiochem Eur. J. Chem. Biol.* **2015**, *16* (16), 2289–2293. <https://doi.org/10.1002/cbic.201500441>.
- (32) Räder, A. F. B.; Weinmüller, M.; Reichart, F.; Schumacher-Klinger, A.; Merzbach, S.; Gilon, C.; Hoffman, A.; Kessler, H. Orally Active Peptides: Is There a Magic Bullet? *Angew. Chem. Int. Ed Engl.* **2018**, *57* (44), 14414–14438. <https://doi.org/10.1002/anie.201807298>.
- (33) Villar, E. A.; Beglov, D.; Chennamadhavuni, S.; Porco, J. A.; Kozakov, D.; Vajda, S.; Whitty, A. How Proteins Bind Macrocycles. *Nat. Chem. Biol.* **2014**, *10* (9), 723–731. <https://doi.org/10.1038/nchembio.1584>.
- (34) Vinogradov, A. A.; Yin, Y.; Suga, H. Macrocyclic Peptides as Drug Candidates: Recent Progress and Remaining Challenges. *J. Am. Chem. Soc.* **2019**, *141* (10), 4167–4181. <https://doi.org/10.1021/jacs.8b13178>.
- (35) Driggers, E. M.; Hale, S. P.; Lee, J.; Terrett, N. K. The Exploration of Macrocycles for Drug Discovery--an Underexploited Structural Class. *Nat. Rev. Drug Discov.* **2008**, *7* (7), 608–624. <https://doi.org/10.1038/nrd2590>.
- (36) Mallinson, J.; Collins, I. Macrocycles in New Drug Discovery. *Future Med. Chem.* **2012**, *4* (11), 1409–1438. <https://doi.org/10.4155/fmc.12.93>.
- (37) Whitty, A.; Viarengo, L. A.; Zhong, M. Progress towards the Broad Use of Non-Peptide Synthetic Macrocycles in Drug Discovery. *Org. Biomol. Chem.* **2017**, *15* (37), 7729–7735. <https://doi.org/10.1039/C7OB00056A>.
- (38) Dharanipragada, R. New Modalities in Conformationally Constrained Peptides for Potency, Selectivity and Cell Permeation. *Future Med. Chem.* **2013**, *5* (7), 831–849. <https://doi.org/10.4155/fmc.13.25>.

- (39) Lau, Y. H.; de Andrade, P.; Wu, Y.; Spring, D. R. Peptide Stapling Techniques Based on Different Macrocyclisation Chemistries. *Chem. Soc. Rev.* **2015**, *44* (1), 91–102. <https://doi.org/10.1039/c4cs00246f>.
- (40) Ngambenjwong, C.; Pineda, J. M. B.; Pun, S. H. Engineering an Affinity-Enhanced Peptide through Optimization of Cyclization Chemistry. *Bioconjug. Chem.* **2016**, *27* (12), 2854–2862. <https://doi.org/10.1021/acs.bioconjchem.6b00502>.
- (41) Skowron, K. J.; Speltz, T. E.; Moore, T. W. Recent Structural Advances in Constrained Helical Peptides. *Med. Res. Rev.* **2019**, *39* (2), 749–770. <https://doi.org/10.1002/med.21540>.
- (42) Tang, J.; He, Y.; Chen, H.; Sheng, W.; Wang, H. Synthesis of Bioactive and Stabilized Cyclic Peptides by Macrocyclization Using C(Sp³)-H Activation. *Chem. Sci.* **2017**, *8* (6), 4565–4570. <https://doi.org/10.1039/c6sc05530c>.
- (43) White, C. J.; Yudin, A. K. Contemporary Strategies for Peptide Macrocyclization. *Nat. Chem.* **2011**, *3* (7), 509–524. <https://doi.org/10.1038/nchem.1062>.
- (44) Felix, A. M.; Heimer, E. P.; Wang, C. T.; Lambros, T. J.; Fournier, A.; Mowles, T. F.; Maines, S.; Campbell, R. M.; Wegrzynski, B. B.; Toome, V. Synthesis, Biological Activity and Conformational Analysis of Cyclic GRF Analogs. *Int. J. Pept. Protein Res.* **1988**, *32* (6), 441–454. <https://doi.org/10.1111/j.1399-3011.1988.tb01375.x>.
- (45) Taylor, J. W. The Synthesis and Study of Side-Chain Lactam-Bridged Peptides. *Biopolymers* **2002**, *66* (1), 49–75. <https://doi.org/10.1002/bip.10203>.
- (46) Blackwell, H. E.; Grubbs, R. H. Highly Efficient Synthesis of Covalently Cross-Linked Peptide Helices by Ring-Closing Metathesis. *Angew. Chem. Int. Ed Engl.* **1998**, *37* (23), 3281–3284. [https://doi.org/10.1002/\(SICI\)1521-3773\(19981217\)37:23<3281::AID-ANIE3281>3.0.CO;2-V](https://doi.org/10.1002/(SICI)1521-3773(19981217)37:23<3281::AID-ANIE3281>3.0.CO;2-V).
- (47) Kim, Y.-W.; Grossmann, T. N.; Verdine, G. L. Synthesis of All-Hydrocarbon Stapled α -Helical Peptides by Ring-Closing Olefin Metathesis. *Nat. Protoc.* **2011**, *6* (6), 761–771. <https://doi.org/10.1038/nprot.2011.324>.
- (48) Verdine, G. L.; Hilinski, G. J. All-Hydrocarbon Stapled Peptides as Synthetic Cell-Accessible Mini-Proteins. *Drug Discov. Today Technol.* **2012**, *9* (1), e41–e47. <https://doi.org/10.1016/j.ddtec.2012.01.004>.
- (49) Bernal, F.; Tyler, A. F.; Korsmeyer, S. J.; Walensky, L. D.; Verdine, G. L. Reactivation of the P53 Tumor Suppressor Pathway by a Stapled P53 Peptide. *J. Am. Chem. Soc.* **2007**, *129* (9), 2456–2457. <https://doi.org/10.1021/ja0693587>.
- (50) Bird, G. H.; Madani, N.; Perry, A. F.; Princiotta, A. M.; Supko, J. G.; He, X.; Gavathiotis, E.; Sodroski, J. G.; Walensky, L. D. Hydrocarbon Double-Stapling Remedies the Proteolytic Instability of a Lengthy Peptide Therapeutic. *Proc. Natl. Acad. Sci. U. S. A.* **2010**, *107* (32), 14093–14098. <https://doi.org/10.1073/pnas.1002713107>.
- (51) Danial, N. N.; Walensky, L. D.; Zhang, C.-Y.; Choi, C. S.; Fisher, J. K.; Molina, A. J. A.; Datta, S. R.; Pitter, K. L.; Bird, G. H.; Wikstrom, J. D.; Deeney, J. T.; Robertson, K.; Morash, J.; Kulkarni, A.; Neschen, S.; Kim, S.; Greenberg, M. E.; Corkey, B. E.; Shirihai, O. S.; Shulman, G. I.; Lowell, B. B.; Korsmeyer, S. J. Dual Role of Proapoptotic BAD in Insulin Secretion and Beta Cell Survival. *Nat. Med.* **2008**, *14* (2), 144–153. <https://doi.org/10.1038/nm1717>.
- (52) Lawrence, J.; Jourdan, M.; Vallée, Y.; Blandin, V. Peptide Cyclization via Ring-Closing Metathesis: The N-Alkenoxy Peptide Approach. *Org. Biomol. Chem.* **2008**, *6* (24), 4575–4581. <https://doi.org/10.1039/B812611A>.
- (53) Sviridov, D.; Ikpot, I.; Stonik, J.; Drake, S.; Amar, M.; Osei-Hwedieh, D.; Piszczek, G.; Turner, S.; Remaley, A. Helix Stabilization of Amphipathic Peptides by Hydrocarbon Stapling Increases Cholesterol Efflux by the ABCA1 Transporter. *Biochem. Biophys. Res. Commun.* **2011**, *410* (3), 446–451. <https://doi.org/10.1016/j.bbrc.2011.05.154>.
- (54) Walensky, L. D.; Kung, A. L.; Escher, I.; Malia, T. J.; Barbuto, S.; Wright, R. D.; Wagner, G.; Verdine, G. L.; Korsmeyer, S. J. Activation of Apoptosis in Vivo by a Hydrocarbon-Stapled BH3 Helix. *Science* **2004**, *305* (5689), 1466–1470. <https://doi.org/10.1126/science.1099191>.
- (55) Zhang, H.; Zhao, Q.; Bhattacharya, S.; Waheed, A. A.; Tong, X.; Hong, A.; Heck, S.; Curreli, F.; Goger, M.; Cowburn, D.; Freed, E. O.; Debnath, A. K. A Cell-Penetrating Helical Peptide

- as a Potential HIV-1 Inhibitor. *J. Mol. Biol.* **2008**, *378* (3), 565–580. <https://doi.org/10.1016/j.jmb.2008.02.066>.
- (56) Rostovtsev, V. V.; Green, L. G.; Fokin, V. V.; Sharpless, K. B. A Stepwise Huisgen Cycloaddition Process: Copper(I)-Catalyzed Regioselective “Ligation” of Azides and Terminal Alkynes. *Angew. Chem. Int. Ed Engl.* **2002**, *41* (14), 2596–2599. [https://doi.org/10.1002/1521-3773\(20020715\)41:14<2596::AID-ANIE2596>3.0.CO;2-4](https://doi.org/10.1002/1521-3773(20020715)41:14<2596::AID-ANIE2596>3.0.CO;2-4).
- (57) Tornøe, C. W.; Christensen, C.; Meldal, M. Peptidotriazoles on Solid Phase: [1,2,3]-Triazoles by Regiospecific Copper(I)-Catalyzed 1,3-Dipolar Cycloadditions of Terminal Alkynes to Azides. *J. Org. Chem.* **2002**, *67* (9), 3057–3064. <https://doi.org/10.1021/jo011148j>.
- (58) Kolb, H. C.; Finn, M. G.; Sharpless, K. B. Click Chemistry: Diverse Chemical Function from a Few Good Reactions. *Angew. Chem. Int. Ed Engl.* **2001**, *40* (11), 2004–2021. [https://doi.org/10.1002/1521-3773\(20010601\)40:11<2004::aid-anie2004>3.3.co;2-x](https://doi.org/10.1002/1521-3773(20010601)40:11<2004::aid-anie2004>3.3.co;2-x).
- (59) Cantel, S.; Isaad, A. L. C.; Scrima, M.; Levy, J. J.; DiMarchi, R. D.; Rovero, P.; Halperin, J. A.; D’Ursi, A. M.; Papini, A. M.; Chorev, M. Synthesis and Conformational Analysis of a Cyclic Peptide Obtained via i to I+4 Intramolecular Side-Chain to Side-Chain Azide-Alkyne 1,3-Dipolar Cycloaddition. *J. Org. Chem.* **2008**, *73* (15), 5663–5674. <https://doi.org/10.1021/jo800142s>.
- (60) Scrima, M.; Chevalier-Isaad, A. L.; Rovero, P.; Papini, A. M.; Chorev, M.; D’Ursi, A. M. CuI-Catalyzed Azide–Alkyne Intramolecular i-to-(I+4) Side-Chain-to-Side-Chain Cyclization Promotes the Formation of Helix-Like Secondary Structures. *Eur. J. Org. Chem.* **2010**, *2010* (3), 446–457. <https://doi.org/10.1002/ejoc.200901157>.
- (61) Kawamoto, S. A.; Coleska, A.; Ran, X.; Yi, H.; Yang, C.-Y.; Wang, S. Design of Triazole-Stapled BCL9 α -Helical Peptides to Target the β -Catenin/B-Cell CLL/Lymphoma 9 (BCL9) Protein-Protein Interaction. *J. Med. Chem.* **2012**, *55* (3), 1137–1146. <https://doi.org/10.1021/jm201125d>.
- (62) Madden, M. M.; Muppidi, A.; Li, Z.; Li, X.; Chen, J.; Lin, Q. Synthesis of Cell-Permeable Stapled Peptide Dual Inhibitors of the P53-Mdm2/Mdmx Interactions via Photoinduced Cycloaddition. *Bioorg. Med. Chem. Lett.* **2011**, *21* (5), 1472–1475. <https://doi.org/10.1016/j.bmcl.2011.01.004>.
- (63) Tian, Y.; Li, J.; Zhao, H.; Zeng, X.; Wang, D.; Liu, Q.; Niu, X.; Huang, X.; Xu, N.; Li, Z. Stapling of Unprotected Helical Peptides via Photo-Induced Intramolecular Thiol-Yne Hydrothiolation. *Chem. Sci.* **2016**, *7* (5), 3325–3330. <https://doi.org/10.1039/c6sc00106h>.
- (64) Wang, Y.; Bruno, B. J.; Cornillie, S.; Nogueira, J. M.; Chen, D.; Cheatham, T. E.; Lim, C. S.; Chou, D. H.-C. Application of Thiol-Yne/Thiol-Ene Reactions for Peptide and Protein Macrocyclizations. *Chem. Weinh. Bergstr. Ger.* **2017**, *23* (29), 7087–7092. <https://doi.org/10.1002/chem.201700572>.
- (65) Wang, Y.; Chou, D. H.-C. A Thiol-Ene Coupling Approach to Native Peptide Stapling and Macrocyclization. *Angew. Chem. Int. Ed Engl.* **2015**, *54* (37), 10931–10934. <https://doi.org/10.1002/anie.201503975>.
- (66) Zhao, B.; Zhang, Q.; Li, Z. Constructing Thioether-Tethered Cyclic Peptides via on-Resin Intra-Molecular Thiol-Ene Reaction. *J. Pept. Sci. Off. Publ. Eur. Pept. Soc.* **2016**, *22* (8), 540–544. <https://doi.org/10.1002/psc.2902>.
- (67) Fadzen, C. M.; Wolfe, J. M.; Cho, C.-F.; Chiocca, E. A.; Lawler, S. E.; Pentelute, B. L. Perfluoroarene-Based Peptide Macrocycles to Enhance Penetration Across the Blood-Brain Barrier. *J. Am. Chem. Soc.* **2017**, *139* (44), 15628–15631. <https://doi.org/10.1021/jacs.7b09790>.
- (68) Jo, H.; Meinhardt, N.; Wu, Y.; Kulkarni, S.; Hu, X.; Low, K. E.; Davies, P. L.; DeGrado, W. F.; Greenbaum, D. C. Development of α -Helical Calpain Probes by Mimicking a Natural Protein-Protein Interaction. *J. Am. Chem. Soc.* **2012**, *134* (42), 17704–17713. <https://doi.org/10.1021/ja307599z>.
- (69) Peraro, L.; Siegert, T. R.; Kritzer, J. A. Conformational Restriction of Peptides Using Dithiol Bis-Alkylation. *Methods Enzymol.* **2016**, *580*, 303–332. <https://doi.org/10.1016/bs.mie.2016.05.035>.

- (70) Rojas, A. J.; Pentelute, B. L.; Buchwald, S. L. Water-Soluble Palladium Reagents for Cysteine S-Arylation under Ambient Aqueous Conditions. *Org. Lett.* **2017**, *19* (16), 4263–4266. <https://doi.org/10.1021/acs.orglett.7b01911>.
- (71) Rojas, A. J.; Zhang, C.; Vinogradova, E. V.; Buchwald, N. H.; Reilly, J.; Pentelute, B. L.; Buchwald, S. L. Divergent Unprotected Peptide Macrocyclisation by Palladium-Mediated Cysteine Arylation. *Chem. Sci.* **2017**, *8* (6), 4257–4263. <https://doi.org/10.1039/c6sc05454d>.
- (72) Spokoyny, A. M.; Zou, Y.; Ling, J. J.; Yu, H.; Lin, Y.-S.; Pentelute, B. L. A Perfluoroaryl-Cysteine S(N)Ar Chemistry Approach to Unprotected Peptide Stapling. *J. Am. Chem. Soc.* **2013**, *135* (16), 5946–5949. <https://doi.org/10.1021/ja400119t>.
- (73) Vinogradova, E. V.; Zhang, C.; Spokoyny, A. M.; Pentelute, B. L.; Buchwald, S. L. Organometallic Palladium Reagents for Cysteine Bioconjugation. *Nature* **2015**, *526* (7575), 687–691. <https://doi.org/10.1038/nature15739>.
- (74) Chen, S.; Morales-Sanfrutos, J.; Angelini, A.; Cutting, B.; Heinis, C. Structurally Diverse Cyclisation Linkers Impose Different Backbone Conformations in Bicyclic Peptides. *Chembiochem Eur. J. Chem. Biol.* **2012**, *13* (7), 1032–1038. <https://doi.org/10.1002/cbic.201200049>.
- (75) Timmerman, P.; Beld, J.; Puijk, W. C.; Meloen, R. H. Rapid and Quantitative Cyclization of Multiple Peptide Loops onto Synthetic Scaffolds for Structural Mimicry of Protein Surfaces. *Chembiochem Eur. J. Chem. Biol.* **2005**, *6* (5), 821–824. <https://doi.org/10.1002/cbic.200400374>.
- (76) Diderich, P.; Bertoldo, D.; Dessen, P.; Khan, M. M.; Pizzitola, I.; Held, W.; Huelsken, J.; Heinis, C. Phage Selection of Chemically Stabilized α -Helical Peptide Ligands. *ACS Chem. Biol.* **2016**, *11* (5), 1422–1427. <https://doi.org/10.1021/acscchembio.5b00963>.
- (77) Kale, S. S.; Villequey, C.; Kong, X.-D.; Zorzi, A.; Deyle, K.; Heinis, C. Cyclization of Peptides with Two Chemical Bridges Affords Large Scaffold Diversities. *Nat. Chem.* **2018**, *10* (7), 715–723. <https://doi.org/10.1038/s41557-018-0042-7>.
- (78) Kong, X.-D.; Moriya, J.; Carle, V.; Pojer, F.; Abriata, L. A.; Deyle, K.; Heinis, C. De Novo Development of Proteolytically Resistant Therapeutic Peptides for Oral Administration. *Nat. Biomed. Eng.* **2020**, *4* (5), 560–571. <https://doi.org/10.1038/s41551-020-0556-3>.
- (79) Baeriswyl, V.; Heinis, C. Phage Selection of Cyclic Peptide Antagonists with Increased Stability toward Intestinal Proteases. *Protein Eng. Des. Sel. PEDS* **2013**, *26* (1), 81–89. <https://doi.org/10.1093/protein/gzs085>.
- (80) Bernhagen, D.; Jungbluth, V.; Quilis, N. G.; Dostalek, J.; White, P. B.; Jalink, K.; Timmerman, P. Bicyclic RGD Peptides with Exquisite Selectivity for the Integrin $\text{Av}\beta 3$ Receptor Using a “Random Design” Approach. *ACS Comb. Sci.* **2019**, *21* (3), 198–206. <https://doi.org/10.1021/acscombsci.8b00144>.
- (81) Heinis, C.; Rutherford, T.; Freund, S.; Winter, G. Phage-Encoded Combinatorial Chemical Libraries Based on Bicyclic Peptides. *Nat. Chem. Biol.* **2009**, *5* (7), 502–507. <https://doi.org/10.1038/nchembio.184>.
- (82) Dang, B.; Wu, H.; Mulligan, V. K.; Mravic, M.; Wu, Y.; Lemmin, T.; Ford, A.; Silva, D.-A.; Baker, D.; DeGrado, W. F. De Novo Design of Covalently Constrained Mesosize Protein Scaffolds with Unique Tertiary Structures. *Proc. Natl. Acad. Sci.* **2017**, *114* (41), 10852–10857. <https://doi.org/10.1073/pnas.1710695114>.
- (83) Neubacher, S.; Saya, J. M.; Amore, A.; Grossmann, T. N. In Situ Cyclization of Proteins (INCYPRO): Cross-Link Derivatization Modulates Protein Stability. *J. Org. Chem.* **2019**. <https://doi.org/10.1021/acs.joc.9b02490>.
- (84) Pelay-Gimeno, M.; Bange, T.; Hennig, S.; Grossmann, T. N. In Situ Cyclization of Native Proteins: Structure-Based Design of a Bicyclic Enzyme. *Angew. Chem. Int. Ed Engl.* **2018**, *57* (35), 11164–11170. <https://doi.org/10.1002/anie.201804506>.
- (85) Blackwell, H. E.; Sadowsky, J. D.; Howard, R. J.; Sampson, J. N.; Chao, J. A.; Steinmetz, W. E.; O’Leary, D. J.; Grubbs, R. H. Ring-Closing Metathesis of Olefinic Peptides: Design, Synthesis, and Structural Characterization of Macrocyclic Helical Peptides. *J. Org. Chem.* **2001**, *66* (16), 5291–5302. <https://doi.org/10.1021/jo015533k>.

- (86) Galande, A. K.; Bramlett, K. S.; Trent, J. O.; Burris, T. P.; Wittliff, J. L.; Spatola, A. F. Potent Inhibitors of LXXLL-Based Protein-Protein Interactions. *Chembiochem Eur. J. Chem. Biol.* **2005**, *6* (11), 1991–1998. <https://doi.org/10.1002/cbic.200500083>.
- (87) Harrison, R. S.; Shepherd, N. E.; Hoang, H. N.; Ruiz-Gómez, G.; Hill, T. A.; Driver, R. W.; Desai, V. S.; Young, P. R.; Abbenante, G.; Fairlie, D. P. Downsizing Human, Bacterial, and Viral Proteins to Short Water-Stable Alpha Helices That Maintain Biological Potency. *Proc. Natl. Acad. Sci. U. S. A.* **2010**, *107* (26), 11686–11691. <https://doi.org/10.1073/pnas.1002498107>.
- (88) Jackson, D. Y.; King, D. S.; Chmielewski, J.; Singh, S.; Schultz, P. G. General Approach to the Synthesis of Short .Alpha.-Helical Peptides. *J. Am. Chem. Soc.* **1991**, *113* (24), 9391–9392. <https://doi.org/10.1021/ja00024a067>.
- (89) Leduc, A.-M.; Trent, J. O.; Wittliff, J. L.; Bramlett, K. S.; Briggs, S. L.; Chirgadze, N. Y.; Wang, Y.; Burris, T. P.; Spatola, A. F. Helix-Stabilized Cyclic Peptides as Selective Inhibitors of Steroid Receptor-Coactivator Interactions. *Proc. Natl. Acad. Sci. U. S. A.* **2003**, *100* (20), 11273–11278. <https://doi.org/10.1073/pnas.1934759100>.
- (90) Phelan, J. C.; Skelton, N. J.; Braisted, A. C.; McDowell, R. S. A General Method for Constraining Short Peptides to an α -Helical Conformation. *J. Am. Chem. Soc.* **1997**, *119* (3), 455–460. <https://doi.org/10.1021/ja9611654>.
- (91) Schafmeister, C. E.; Po, J.; Verdine, G. L. An All-Hydrocarbon Cross-Linking System for Enhancing the Helicity and Metabolic Stability of Peptides. *J. Am. Chem. Soc.* **2000**, *122* (24), 5891–5892. <https://doi.org/10.1021/ja000563a>.
- (92) Pelay-Gimeno, M.; Glas, A.; Koch, O.; Grossmann, T. N. Structure-Based Design of Inhibitors of Protein–Protein Interactions: Mimicking Peptide Binding Epitopes. *Angew. Chem. Int. Ed Engl.* **2015**, *54* (31), 8896–8927. <https://doi.org/10.1002/anie.201412070>.
- (93) Bhardwaj, G.; Mulligan, V. K.; Bahl, C. D.; Gilmore, J. M.; Harvey, P. J.; Cheneval, O.; Buchko, G. W.; Pulavarti, S. V. S. R. K.; Kaas, Q.; Eletsky, A.; Huang, P.-S.; Johnsen, W. A.; Greisen, P.; Rocklin, G. J.; Song, Y.; Linsky, T. W.; Watkins, A.; Rettie, S. A.; Xu, X.; Carter, L. P.; Bonneau, R.; Olson, J. M.; Coutsiias, E.; Correnti, C. E.; Szyperski, T.; Craik, D. J.; Baker, D. Accurate de Novo Design of Hyperstable Constrained Peptides. *Nature* **2016**, *538* (7625), 329–335. <https://doi.org/10.1038/nature19791>.
- (94) Est, C. B.; Mangrolia, P.; Murphy, R. M. ROSETTA-Informed Design of Structurally Stabilized Cyclic Anti-Amyloid Peptides. *Protein Eng. Des. Sel.* **2019**, *32* (2), 47–57. <https://doi.org/10.1093/protein/gzz016>.
- (95) Guéret, S. M.; Thavam, S.; Carbajo, R. J.; Potowski, M.; Larsson, N.; Dahl, G.; Dellsén, A.; Grossmann, T. N.; Plowright, A. T.; Valeur, E.; Lemurell, M.; Waldmann, H. Macrocyclic Modalities Combining Peptide Epitopes and Natural Product Fragments. *J. Am. Chem. Soc.* **2020**. <https://doi.org/10.1021/jacs.0c00269>.
- (96) Mulligan, V. K. The Emerging Role of Computational Design in Peptide Macrocyclic Drug Discovery. *Expert Opin. Drug Discov.* **2020**, *0* (0), 1–19. <https://doi.org/10.1080/17460441.2020.1751117>.
- (97) Bonnet, P.; Agrafiotis, D. K.; Zhu, F.; Martin, E. Conformational Analysis of Macrocycles: Finding What Common Search Methods Miss. *J. Chem. Inf. Model.* **2009**, *49* (10), 2242–2259. <https://doi.org/10.1021/ci900238a>.
- (98) Chen, I.-J.; Foloppe, N. Tackling the Conformational Sampling of Larger Flexible Compounds and Macrocycles in Pharmacology and Drug Discovery. *Bioorg. Med. Chem.* **2013**, *21* (24), 7898–7920. <https://doi.org/10.1016/j.bmc.2013.10.003>.
- (99) Coutsiias, E. A.; Lexa, K. W.; Wester, M. J.; Pollock, S. N.; Jacobson, M. P. Exhaustive Conformational Sampling of Complex Fused Ring Macrocycles Using Inverse Kinematics. *J. Chem. Theory Comput.* **2016**, *12* (9), 4674–4687. <https://doi.org/10.1021/acs.jctc.6b00250>.
- (100) Geng, H.; Jiang, F.; Wu, Y.-D. Accurate Structure Prediction and Conformational Analysis of Cyclic Peptides with Residue-Specific Force Fields. *J. Phys. Chem. Lett.* **2016**, *7* (10), 1805–1810. <https://doi.org/10.1021/acs.jpcllett.6b00452>.

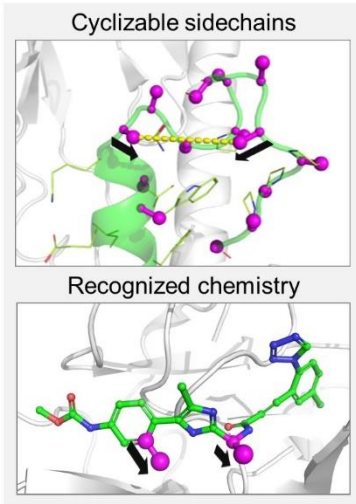
- (101) Gil-Ley, A.; Bussi, G. Enhanced Conformational Sampling Using Replica Exchange with Collective-Variable Tempering. *J. Chem. Theory Comput.* **2015**, *11* (3), 1077–1085. <https://doi.org/10.1021/ct5009087>.
- (102) Hosseinzadeh, P.; Bhardwaj, G.; Mulligan, V. K.; Shortridge, M. D.; Craven, T. W.; Pardo-Avila, F.; Rettie, S. A.; Kim, D. E.; Silva, D.-A.; Ibrahim, Y. M.; Webb, I. K.; Cort, J. R.; Adkins, J. N.; Varani, G.; Baker, D. Comprehensive Computational Design of Ordered Peptide Macrocycles. *Science* **2017**, *358* (6369), 1461–1466. <https://doi.org/10.1126/science.aap7577>.
- (103) Kamenik, A. S.; Lessel, U.; Fuchs, J. E.; Fox, T.; Liedl, K. R. Peptidic Macrocycles - Conformational Sampling and Thermodynamic Characterization. *J. Chem. Inf. Model.* **2018**, *58* (5), 982–992. <https://doi.org/10.1021/acs.jcim.8b00097>.
- (104) Labute, P. LowModeMD—Implicit Low-Mode Velocity Filtering Applied to Conformational Search of Macrocycles and Protein Loops. *J. Chem. Inf. Model.* **2010**, *50* (5), 792–800. <https://doi.org/10.1021/ci900508k>.
- (105) Olanders, G.; Alogheli, H.; Brandt, P.; Karlén, A. Conformational Analysis of Macrocycles: Comparing General and Specialized Methods. *J. Comput. Aided Mol. Des.* **2020**, *34* (3), 231–252. <https://doi.org/10.1007/s10822-020-00277-2>.
- (106) Sindhikara, D.; Spronk, S. A.; Day, T.; Borrelli, K.; Cheney, D. L.; Posy, S. L. Improving Accuracy, Diversity, and Speed with Prime Macrocycle Conformational Sampling. *J. Chem. Inf. Model.* **2017**, *57* (8), 1881–1894. <https://doi.org/10.1021/acs.jcim.7b00052>.
- (107) Sindhikara, D.; Borrelli, K. High Throughput Evaluation of Macrocyclization Strategies for Conformer Stabilization. *Sci. Rep.* **2018**, *8*. <https://doi.org/10.1038/s41598-018-24766-5>.
- (108) Watts, K. S.; Dalal, P.; Tebben, A. J.; Cheney, D. L.; Shelley, J. C. Macrocycle Conformational Sampling with MacroModel. *J. Chem. Inf. Model.* **2014**, *54* (10), 2680–2696. <https://doi.org/10.1021/ci5001696>.
- (109) Witek, J.; Keller, B. G.; Blatter, M.; Meissner, A.; Wagner, T.; Riniker, S. Kinetic Models of Cyclosporin A in Polar and Apolar Environments Reveal Multiple Congruent Conformational States. *J. Chem. Inf. Model.* **2016**, *56* (8), 1547–1562. <https://doi.org/10.1021/acs.jcim.6b00251>.
- (110) Allen, S. E.; Dokholyan, N. V.; Bowers, A. A. Dynamic Docking of Conformationally Constrained Macrocycles: Methods and Applications. *ACS Chem. Biol.* **2016**, *11* (1), 10–24. <https://doi.org/10.1021/acscchembio.5b00663>.
- (111) Alogheli, H.; Olanders, G.; Schaal, W.; Brandt, P.; Karlén, A. Docking of Macrocycles: Comparing Rigid and Flexible Docking in Glide. *J. Chem. Inf. Model.* **2017**, *57* (2), 190–202. <https://doi.org/10.1021/acs.jcim.6b00443>.
- (112) Martin, S. J.; Chen, I.-J.; Chan, A. W. E.; Foloppe, N. Modelling the Binding Mode of Macrocycles: Docking and Conformational Sampling. *Bioorg. Med. Chem.* **2020**, *28* (1), 115143. <https://doi.org/10.1016/j.bmc.2019.115143>.
- (113) Glide Schrödinger Release 2019-3 Glide, Schrödinger, LLC, New York, NY, 2019 (accessed Jan 31, 2018).
- (114) Ugur, I.; Schroft, M.; Marion, A.; Glaser, M.; Antes, I. Predicting the Bioactive Conformations of Macrocycles: A Molecular Dynamics-Based Docking Procedure with DynaDock. *J. Mol. Model.* **2019**, *25* (7), 1–13. <https://doi.org/10.1007/s00894-019-4077-5>.
- (115) Wagner, V.; Jantz, L.; Briem, H.; Sommer, K.; Rarey, M.; Christ, C. D. Computational Macrocyclization: From de Novo Macrocycle Generation to Binding Affinity Estimation. *ChemMedChem* **2017**, *12* (22), 1866–1872. <https://doi.org/10.1002/cmdc.201700478>.
- (116) Yu, H. S.; Deng, Y.; Wu, Y.; Sindhikara, D.; Rask, A. R.; Kimura, T.; Abel, R.; Wang, L. Accurate and Reliable Prediction of the Binding Affinities of Macrocycles to Their Protein Targets. *J. Chem. Theory Comput.* **2017**, *13* (12), 6290–6300. <https://doi.org/10.1021/acs.jctc.7b00885>.
- (117) Wallraven, K.; Holmelin, F. L.; Glas, A.; Hennig, S.; Frolov, A. I.; Grossmann, T. N. Adapting Free Energy Perturbation Simulations for Large Macrocyclic Ligands: How to Dissect Contributions from Direct Binding and Free Ligand Flexibility. *Chem. Sci.* **2020**, *11* (8), 2269–2276. <https://doi.org/10.1039/C9SC04705K>.

- (118) Friesner, R. A.; Banks, J. L.; Murphy, R. B.; Halgren, T. A.; Klicic, J. J.; Mainz, D. T.; Repasky, M. P.; Knoll, E. H.; Shelley, M.; Perry, J. K.; Shaw, D. E.; Francis, P.; Shenkin, P. S. Glide: A New Approach for Rapid, Accurate Docking and Scoring. 1. Method and Assessment of Docking Accuracy. *J. Med. Chem.* **2004**, *47* (7), 1739–1749. <https://doi.org/10.1021/jm0306430>.
- (119) Halgren, T. A.; Murphy, R. B.; Friesner, R. A.; Beard, H. S.; Frye, L. L.; Pollard, W. T.; Banks, J. L. Glide: A New Approach for Rapid, Accurate Docking and Scoring. 2. Enrichment Factors in Database Screening. *J. Med. Chem.* **2004**, *47* (7), 1750–1759. <https://doi.org/10.1021/jm030644s>.
- (120) Kollman, P. A.; Massova, I.; Reyes, C.; Kuhn, B.; Huo, S.; Chong, L.; Lee, M.; Lee, T.; Duan, Y.; Wang, W.; Donini, O.; Cieplak, P.; Srinivasan, J.; Case, D. A.; Cheatham, T. E. Calculating Structures and Free Energies of Complex Molecules: Combining Molecular Mechanics and Continuum Models. *Acc. Chem. Res.* **2000**, *33* (12), 889–897. <https://doi.org/10.1021/ar000033j>.
- (121) Srinivasan, J.; Miller, J.; Kollman, P. A.; Case, D. A. Continuum Solvent Studies of the Stability of RNA Hairpin Loops and Helices. *J. Biomol. Struct. Dyn.* **1998**, *16* (3), 671–682. <https://doi.org/10.1080/07391102.1998.10508279>.
- (122) Paulsen, J. L.; Yu, H. S.; Sindhikara, D.; Wang, L.; Appleby, T. C.; Villaseñor, A. G.; Schmitz, U.; Shivakumar, D. Evaluation of Free Energy Calculations for the Prioritization of Macrocyclic Synthesis. *J. Chem. Inf. Model.* **2020**. <https://doi.org/10.1021/acs.jcim.0c00132>.
- (123) Daylight Theory: SMARTS - A Language for Describing Molecular Patterns <https://www.daylight.com/dayhtml/doc/theory/theory.smarts.html> (accessed Apr 6, 2020).
- (124) Evers, A.; Haack, T.; Lorenz, M.; Bossart, M.; Elvert, R.; Henkel, B.; Stengelin, S.; Kurz, M.; Glien, M.; Dudda, A.; Lorenz, K.; Kadereit, D.; Wagner, M. Design of Novel Exendin-Based Dual Glucagon-like Peptide 1 (GLP-1)/Glucagon Receptor Agonists. *J. Med. Chem.* **2017**, *60* (10), 4293–4303. <https://doi.org/10.1021/acs.jmedchem.7b00174>.
- (125) Evers, A.; Bossart, M.; Pfeiffer-Marek, S.; Elvert, R.; Schreuder, H.; Kurz, M.; Stengelin, S.; Lorenz, M.; Herling, A.; Konkar, A.; Lukasczyk, U.; Pfenninger, A.; Lorenz, K.; Haack, T.; Kadereit, D.; Wagner, M. Dual Glucagon-like Peptide 1 (GLP-1)/Glucagon Receptor Agonists Specifically Optimized for Multidose Formulations. *J. Med. Chem.* **2018**, *61* (13), 5580–5593. <https://doi.org/10.1021/acs.jmedchem.8b00292>.
- (126) Prime Schrödinger Release 2019-3 Prime, Schrödinger, LLC, New York, NY, 2019 (accessed Jan 31, 2018).
- (127) Day, J. W.; Ottaway, N.; Patterson, J. T.; Gelfanov, V.; Smiley, D.; Gidda, J.; Findeisen, H.; Bruemmer, D.; Drucker, D. J.; Chaudhary, N.; Holland, J.; Hembree, J.; Abplanalp, W.; Grant, E.; Ruehl, J.; Wilson, H.; Kirchner, H.; Lockie, S. H.; Hofmann, S.; Woods, S. C.; Nogueiras, R.; Pfluger, P. T.; Perez-Tilve, D.; DiMarchi, R.; Tschöp, M. H. A New Glucagon and GLP-1 Co-Agonist Eliminates Obesity in Rodents. *Nat. Chem. Biol.* **2009**, *5* (10), 749–757. <https://doi.org/10.1038/nchembio.209>.
- (128) Miranda, L. P.; Winters, K. A.; Gegg, C. V.; Patel, A.; Aral, J.; Long, J.; Zhang, J.; Diamond, S.; Guido, M.; Stanislaus, S.; Ma, M.; Li, H.; Rose, M. J.; Poppe, L.; Véniant, M. M. Design and Synthesis of Conformationally Constrained Glucagon-like Peptide-1 Derivatives with Increased Plasma Stability and Prolonged in Vivo Activity. *J. Med. Chem.* **2008**, *51* (9), 2758–2765. <https://doi.org/10.1021/jm701522b>.
- (129) Murage, E. N.; Gao, G.; Bisello, A.; Ahn, J.-M. Development of Potent Glucagon-like Peptide-1 Agonists with High Enzyme Stability via Introduction of Multiple Lactam Bridges. *J. Med. Chem.* **2010**, *53* (17), 6412–6420. <https://doi.org/10.1021/jm100602m>.
- (130) Murage, E. N.; Schroeder, J. C.; Beinborn, M.; Ahn, J.-M. Search for Alpha-Helical Propensity in the Receptor-Bound Conformation of Glucagon-like Peptide-1. *Bioorg. Med. Chem.* **2008**, *16* (23), 10106–10112. <https://doi.org/10.1016/j.bmc.2008.10.006>.
- (131) Grossmann, T. N.; Yeh, J. T.-H.; Bowman, B. R.; Chu, Q.; Moellering, R. E.; Verdine, G. L. Inhibition of Oncogenic Wnt Signaling through Direct Targeting of β -Catenin. *Proc. Natl. Acad. Sci.* **2012**, *109* (44), 17942–17947. <https://doi.org/10.1073/pnas.1208396109>.

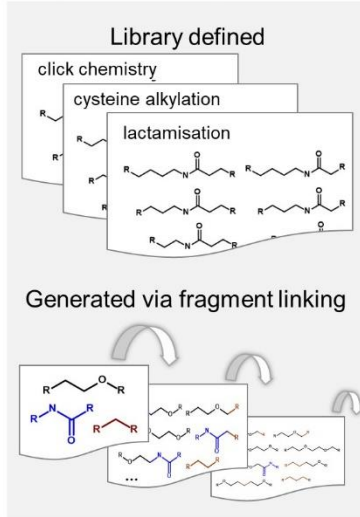
- (132) Schreuder, H.; Liesum, A.; Lönze, P.; Stump, H.; Hoffmann, H.; Schiell, M.; Kurz, M.; Toti, L.; Bauer, A.; Kallus, C.; Klemke-Jahn, C.; Czech, J.; Kramer, D.; Enke, H.; Niedermeyer, T. H. J.; Morrison, V.; Kumar, V.; Brönstrup, M. Isolation, Co-Crystallization and Structure-Based Characterization of Anabaenopeptins as Highly Potent Inhibitors of Activated Thrombin Activatable Fibrinolysis Inhibitor (TAFIa). *Sci. Rep.* **2016**, *6* (1), 1–9. <https://doi.org/10.1038/srep32958>.
- (133) Halland, N.; Brönstrup, M.; Czech, J.; Czechtizky, W.; Evers, A.; Follmann, M.; Kohlmann, M.; Schiell, M.; Kurz, M.; Schreuder, H. A.; Kallus, C. Novel Small Molecule Inhibitors of Activated Thrombin Activatable Fibrinolysis Inhibitor (TAFIa) from Natural Product Anabaenopeptin. *J. Med. Chem.* **2015**, *58* (11), 4839–4844. <https://doi.org/10.1021/jm501840b>.
- (134) Halland, N.; Czech, J.; Czechtizky, W.; Evers, A.; Follmann, M.; Kohlmann, M.; Schreuder, H. A.; Kallus, C. Sulfamide as Zinc Binding Motif in Small Molecule Inhibitors of Activated Thrombin Activatable Fibrinolysis Inhibitor (TAFIa). *J. Med. Chem.* **2016**, *59* (20), 9567–9573. <https://doi.org/10.1021/acs.jmedchem.6b01276>.
- (135) Corte, J. R.; Fang, T.; Osuna, H.; Pinto, D. J. P.; Rossi, K. A.; Myers, J. E.; Sheriff, S.; Lou, Z.; Zheng, J. J.; Harper, T. W.; Bozarth, J. M.; Wu, Y.; Luetzgen, J. M.; Seiffert, D. A.; Decicco, C. P.; Wexler, R. R.; Quan, M. L. Structure-Based Design of Macrocyclic Factor XIa Inhibitors: Discovery of the Macrocyclic Amide Linker. *J. Med. Chem.* **2017**, *60* (3), 1060–1075. <https://doi.org/10.1021/acs.jmedchem.6b01460>.
- (136) Sun, X.; Gao, H.; Yang, Y.; He, M.; Wu, Y.; Song, Y.; Tong, Y.; Rao, Y. PROTACs: Great Opportunities for Academia and Industry. *Signal Transduct. Target. Ther.* **2019**, *4* (1), 1–33. <https://doi.org/10.1038/s41392-019-0101-6>.
- (137) Testa, A.; Hughes, S. J.; Lucas, X.; Wright, J. E.; Ciulli, A. Structure-Based Design of a Macrocyclic PROTAC. *Angew. Chem. Int. Ed.* **2020**, *59* (4), 1727–1734. <https://doi.org/10.1002/anie.201914396>.
- (138) Hughes, S. J.; Ciulli, A. Molecular Recognition of Ternary Complexes: A New Dimension in the Structure-Guided Design of Chemical Degraders. *Essays Biochem.* **2017**, *61* (5), 505–516. <https://doi.org/10.1042/EBC20170041>.
- (139) De Guzman, R. N.; Goto, N. K.; Dyson, H. J.; Wright, P. E. Structural Basis for Cooperative Transcription Factor Binding to the CBP Coactivator. *J. Mol. Biol.* **2006**, *355* (5), 1005–1013. <https://doi.org/10.1016/j.jmb.2005.09.059>.
- (140) Le Roux, A.; Blaise, É.; Boudreault, P.-L.; Comeau, C.; Doucet, A.; Giarrusso, M.; Collin, M.-P.; Neubauer, T.; Kölling, F.; Göller, A. H.; Seep, L.; Tshitenge, D. T.; Wittwer, M.; Kullmann, M.; Hillisch, A.; Mittendorf, J.; Marsault, E. Structure–Permeability Relationship of Semipeptidic Macrocycles—Understanding and Optimizing Passive Permeability and Efflux Ratio. *J. Med. Chem.* **2020**, 6774–6783. <https://doi.org/10.1021/acs.jmedchem.0c00013>.
- (141) Cummings, M. D.; Sekharan, S. Structure-Based Macrocyclic Design in Small-Molecule Drug Discovery and Simple Metrics To Identify Opportunities for Macrocyclization of Small-Molecule Ligands. *J. Med. Chem.* **2019**, *62* (15), 6843–6853. <https://doi.org/10.1021/acs.jmedchem.8b01985>.
- (142) Jorgensen, W. L.; Maxwell, D. S.; Tirado-Rives, J. Development and Testing of the OPLS All-Atom Force Field on Conformational Energetics and Properties of Organic Liquids. *J. Am. Chem. Soc.* **1996**, *118* (45), 11225–11236. <https://doi.org/10.1021/ja9621760>.
- (143) Jorgensen, W. L.; Tirado-Rives, J. The OPLS [Optimized Potentials for Liquid Simulations] Potential Functions for Proteins, Energy Minimizations for Crystals of Cyclic Peptides and Crambin. *J. Am. Chem. Soc.* **1988**, *110* (6), 1657–1666. <https://doi.org/10.1021/ja00214a001>.
- (144) Shivakumar, D.; Harder, E.; Damm, W.; Friesner, R. A.; Sherman, W. Improving the Prediction of Absolute Solvation Free Energies Using the Next Generation OPLS Force Field. *J. Chem. Theory Comput.* **2012**, *8* (8), 2553–2558. <https://doi.org/10.1021/ct300203w>.
- (145) Hoover, null. Canonical Dynamics: Equilibrium Phase-Space Distributions. *Phys. Rev. Gen. Phys.* **1985**, *31* (3), 1695–1697.

- (146) Nosé, S. A Unified Formulation of the Constant Temperature Molecular Dynamics Methods. *J. Chem. Phys.* **1984**, *81* (1), 511–519. <https://doi.org/10.1063/1.447334>.
- (147) Martyna, G. J.; Tobias, D. J.; Klein, M. L. Constant Pressure Molecular Dynamics Algorithms. *J. Chem. Phys.* **1994**, *101* (5), 4177–4189. <https://doi.org/10.1063/1.467468>.
- (148) Darden, T.; York, D.; Pedersen, L. Particle Mesh Ewald: An $N \cdot \log(N)$ Method for Ewald Sums in Large Systems. *J. Chem. Phys.* **1993**, *98* (12), 10089–10092. <https://doi.org/10.1063/1.464397>.
- (149) Ryckaert, J.-P.; Ciccotti, G.; Berendsen, H. J. C. Numerical Integration of the Cartesian Equations of Motion of a System with Constraints: Molecular Dynamics of n-Alkanes. *J. Comput. Phys.* **1977**, *23* (3), 327–341. [https://doi.org/10.1016/0021-9991\(77\)90098-5](https://doi.org/10.1016/0021-9991(77)90098-5).
- (150) King, D. S.; Fields, C. G.; Fields, G. B. A Cleavage Method Which Minimizes Side Reactions Following Fmoc Solid Phase Peptide Synthesis. *Int. J. Pept. Protein Res.* **1990**, *36* (3), 255–266.

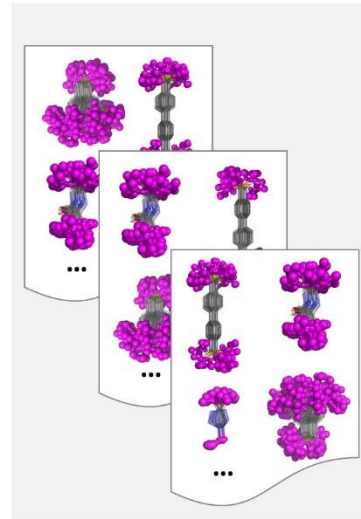
Step 1: Attachment point identification



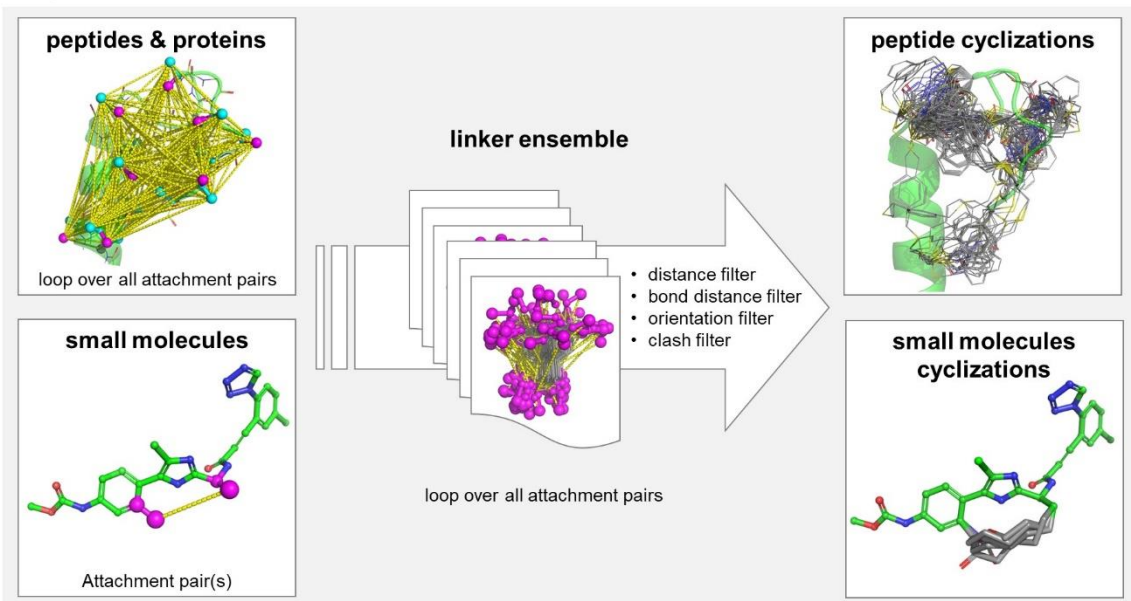
Step 2: Linker generation



Step 3: Linker sampling



Step 4: Combinatorial structure enumeration



Step 5: Scoring

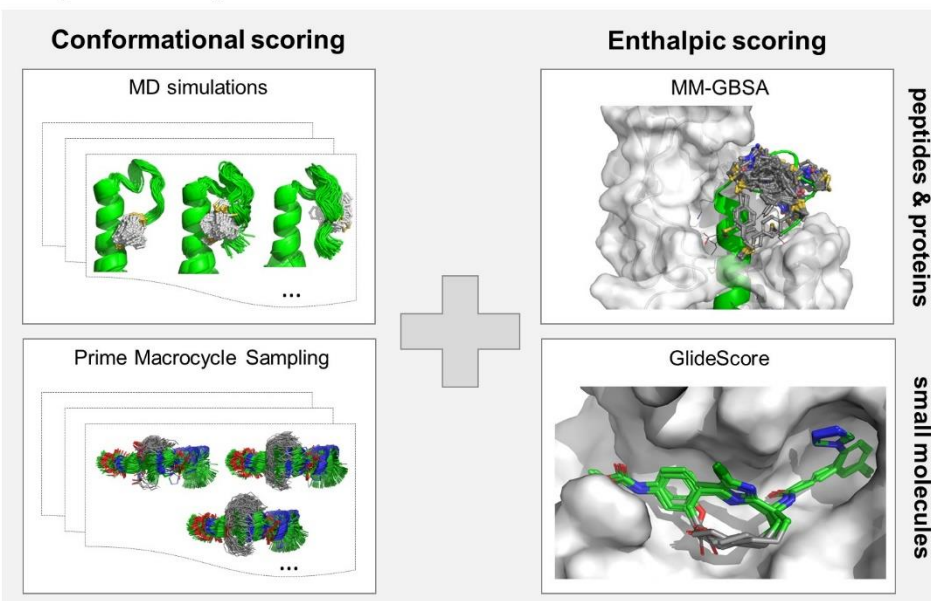


Figure 1. Procedure for the automated design of macrocycles. Step 1) The user prepares a linear starting molecule. The attachment points may be either identified automatically or specified by the user. Step 2) Generation of chemical linkers. These might either be provided as explicit lists, e.g., based on available chemical reagents, or can be grown automatically by combining and enumerating small building fragments. Step 3) A full conformational ensemble of each linker is generated and (step 4) mapped with all attachment points to eliminate unfavourable cyclizations applying different geometric filter criteria. Step 5) Finally, the cyclized ligands are ranked applying conformational and/or enthalpic scoring.

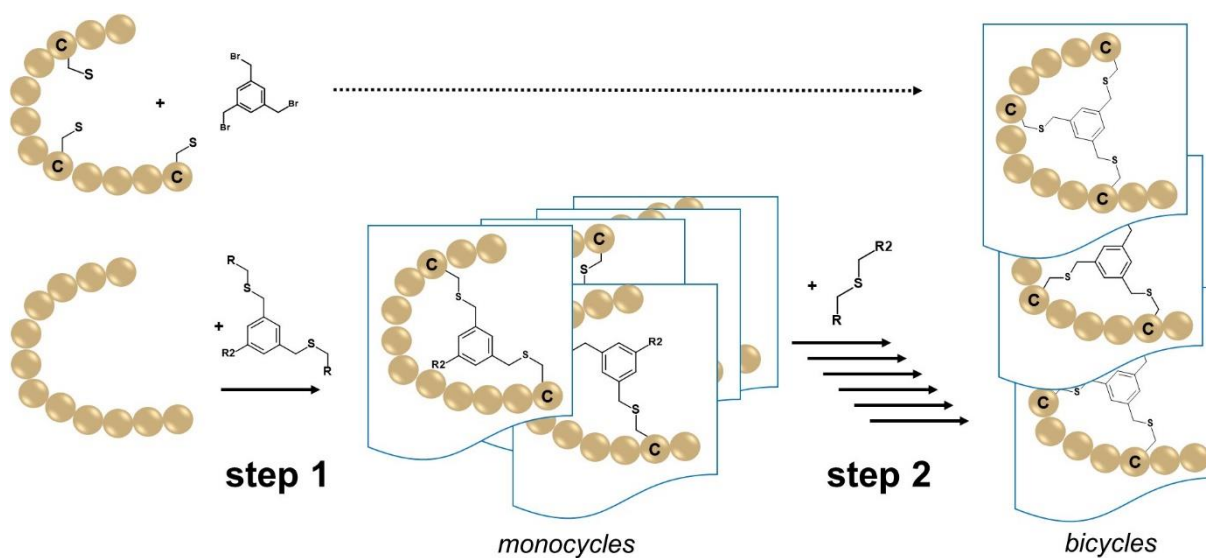
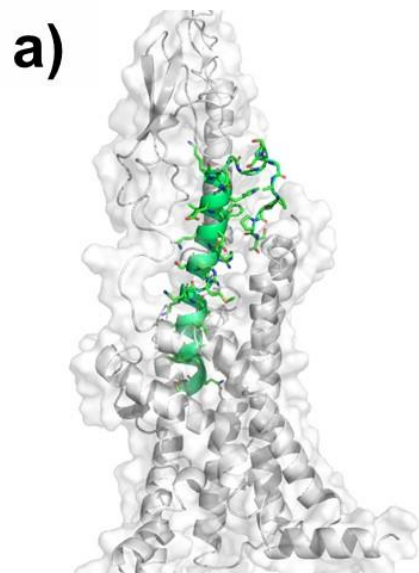
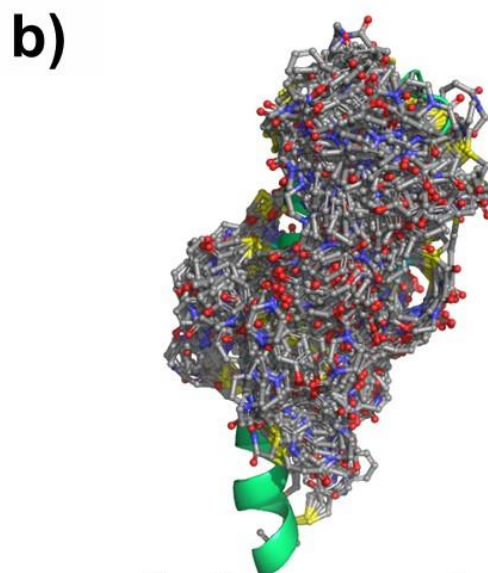


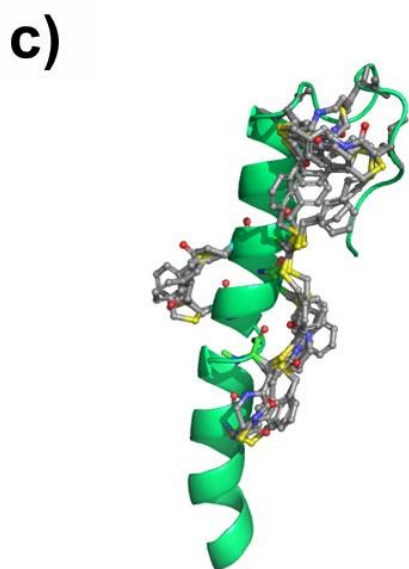
Figure 2. Approach for modeling bicyclic peptide structures using a tri-symmetrical linker. In step 1, all geometrically reasonable monocyclic structures are generated. In the second cyclization routine (step 2), the unlinked (third) attachment point of the linker is evaluated for attachment to the peptide backbone for construction of the second cycle.



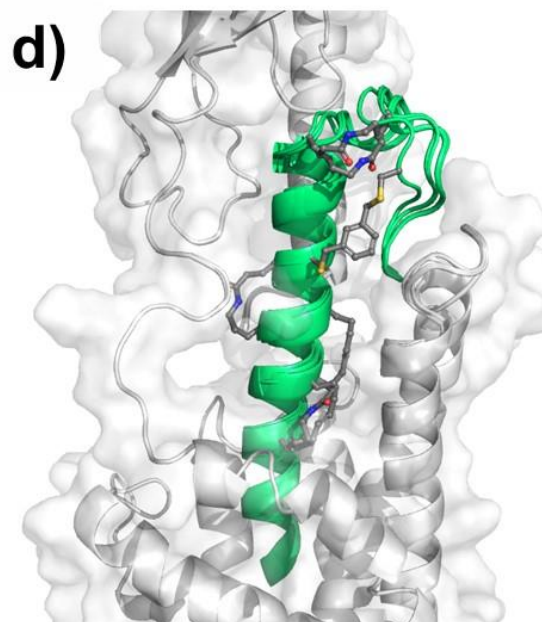
**modelled binding mode of
receptor-peptide complex**



**cyclization proposals
(without constraints)**



**cyclization proposals (focused
library with constraints)**



**predicted binding modes of
synthesized molecules**

Figure 3. Cyclization of dual agonists of the GLP-1 and glucagon receptor. a) Predicted binding mode of the dual agonist **4a** at the GLP-1R (pdb code 5vai). b) Automatically generated cyclization proposals with all chemical linkers shown in Table 1. c) Cyclization proposals using a focused list of reagents and attachment positions. d) Predicted binding modes of synthesized peptides obtained from MM/GBSA energy minimization.

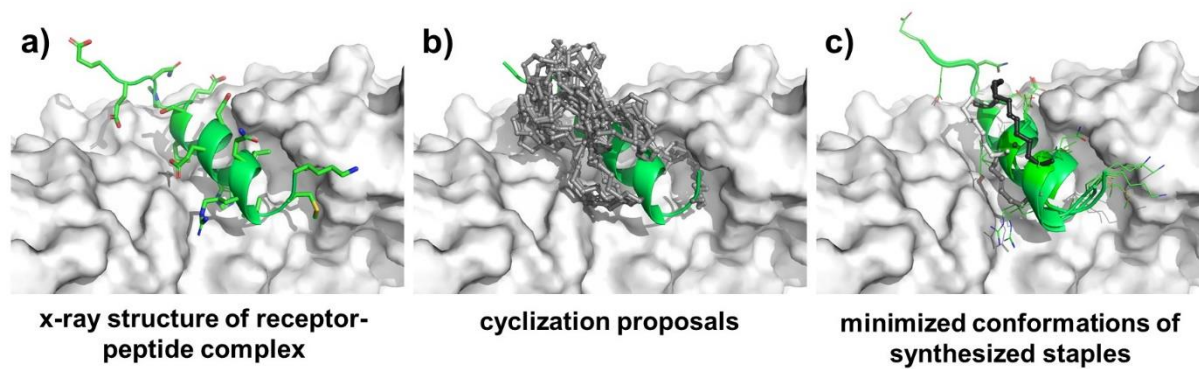


Figure 4. Stapling of a peptidic inhibitor of β -catenin. a) x-ray structure of the receptor-peptide complex (pdb code 1qz7). b) Cyclization proposals that were produced by the algorithm for two different linkers without constraints on stereochemistry. c) Predicted binding modes of **5b-d** obtained from MM/GBSA energy minimization.

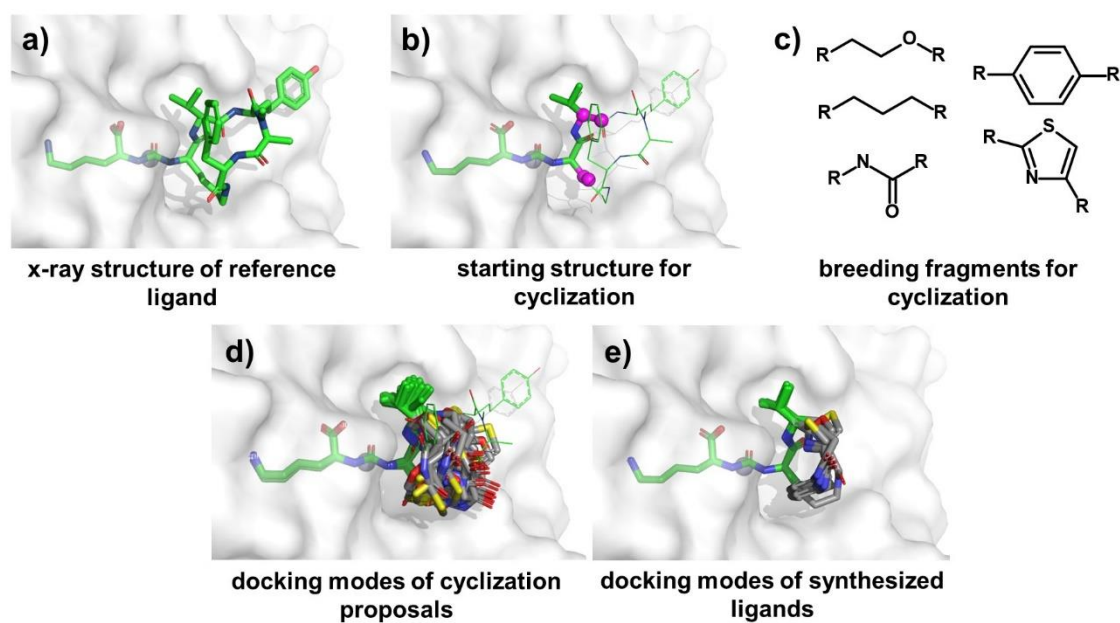


Figure 5. Macrocyclization of a TAF1a inhibitor. a) x-ray structure of anabaenopeptin C in complex with the surrogate protease carboxypeptidase B (pdb code 5lrj). b) Anabaenopeptin C was modified to obtain the starting structure for rescaffolding of the macrocycle. The attachment vectors are indicated in magenta. c) Breeding fragments that were combined and enumerated for cyclization. Predicted binding modes of d) automatically generated cyclization proposals and e) four cyclization proposals that were synthesized and experimentally tested.

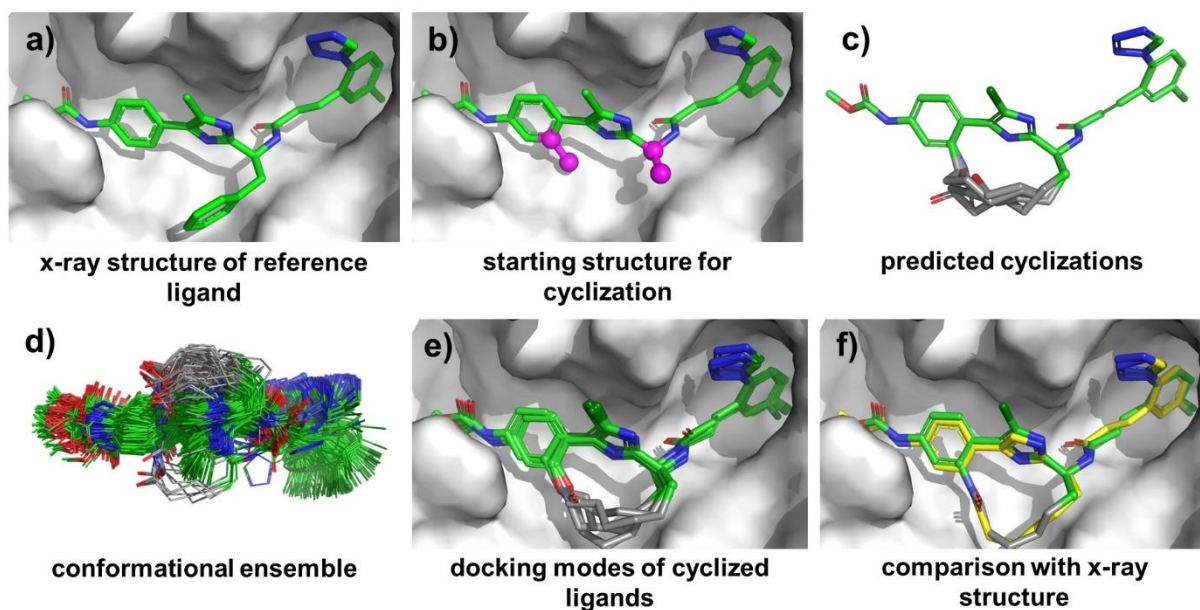


Figure 6. Macrocyclization of a factor XIa inhibitor. a) x-ray structure of acyclic phenyl imidazole lead compound (pdb code 4y8x). b) The lead structure was modified to obtain the starting structure for cyclization. The attachment vectors are indicated in magenta. c) Cyclized conformations of **7a-f** obtained after automated attachment of linkers (see Table 7) to the starting structure. d) Conformational ensemble obtained from Prime-MCS (shown for **7e**). e) Predicted binding modes of **7a-f** obtained from docking with Glide. f) Comparison of predicted binding mode of **7e** with the x-ray structure of a close analogue (pdb code 5tku).

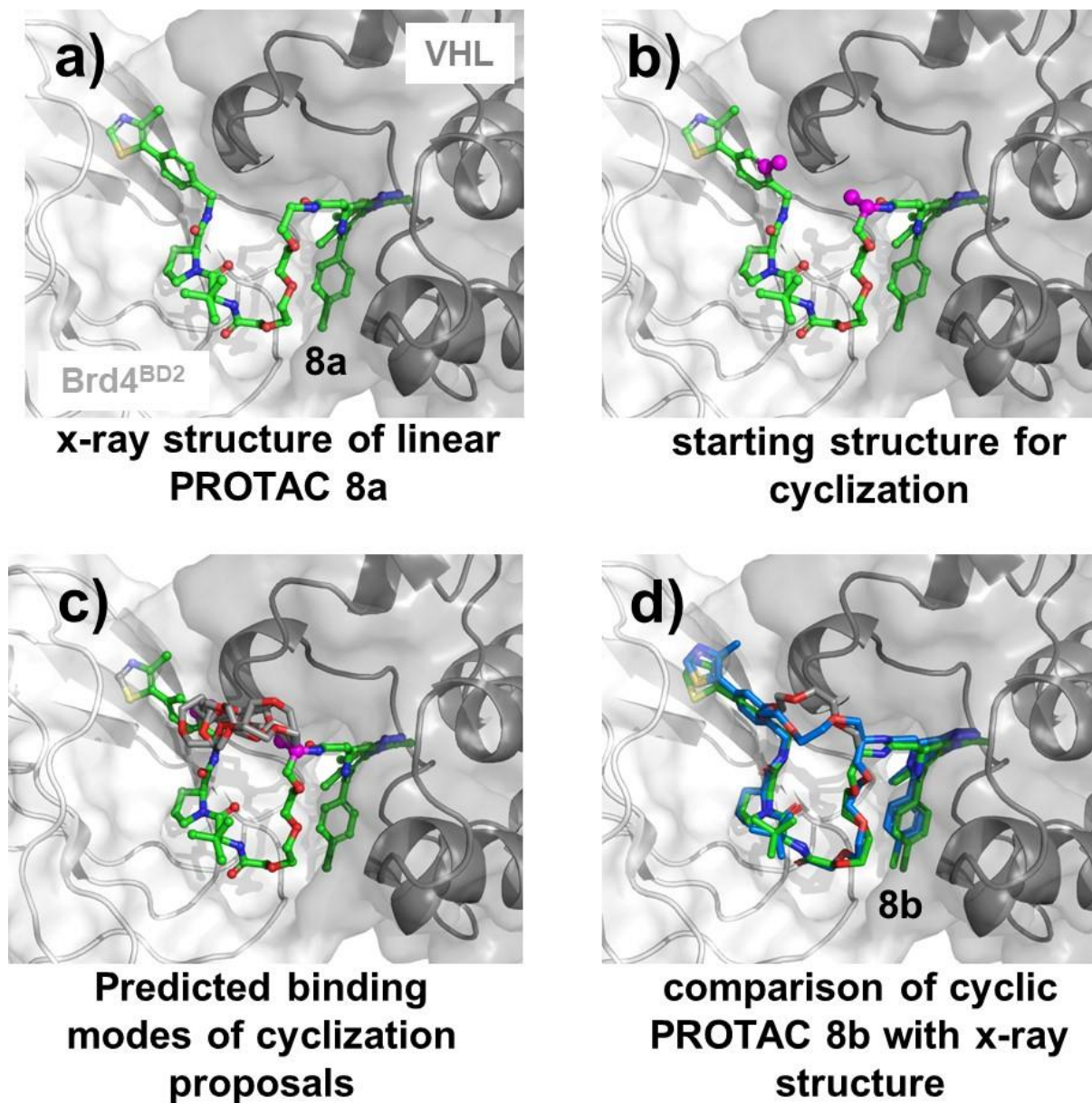


Figure 7. a) x-ray structure of the linear PROTAC MZ1 (**8a**) in complex with Brd4^{BD2} and VHL-EloB-EloC (pdb code 5t35). b) The PROTAC structure was modified to obtain the starting structure for cyclization. The attachment vectors are indicated in magenta. c) Cyclized conformations comprising PEG units of different length, minimized in the protein environment. d) Comparison of predicted binding mode of **8b** with the experimental binding mode (pdb 6sis).

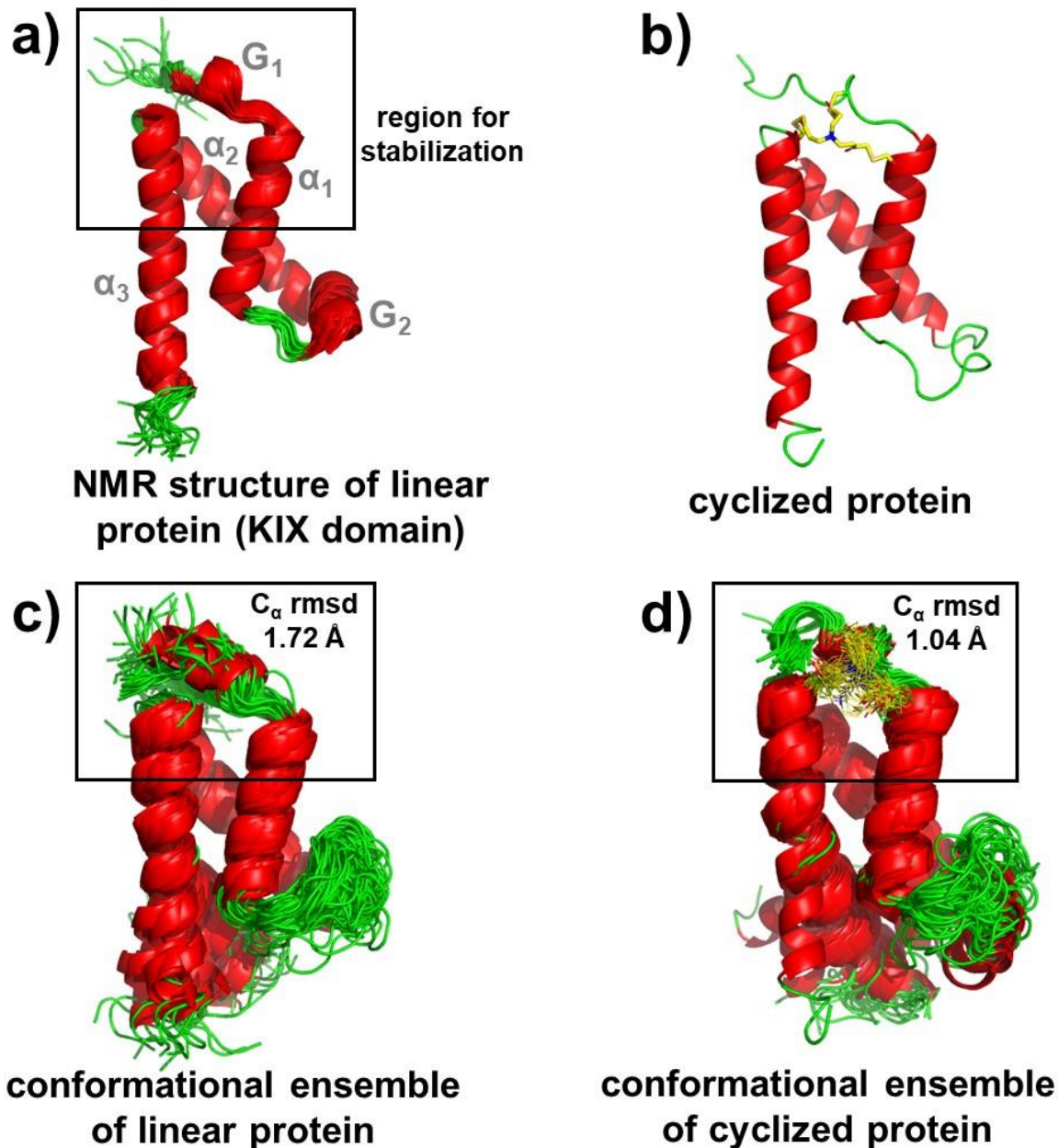


Figure 8. Generation of bicyclic variants of KIX domain from the human CREB binding protein. a) NMR structure of KIX (PDB code 2agh). The junction between the helical bundle (α_1 , α_2 , α_3) and the C-terminal 3_{10} helix (G_1), that was subjected to covalent stabilization, is indicated. b) Cyclized construct that links residues 594, 599 and 646. Figures c) and d) show the 3D alignment of snapshots from 100 ns simulations of the linear and cyclized proteins.

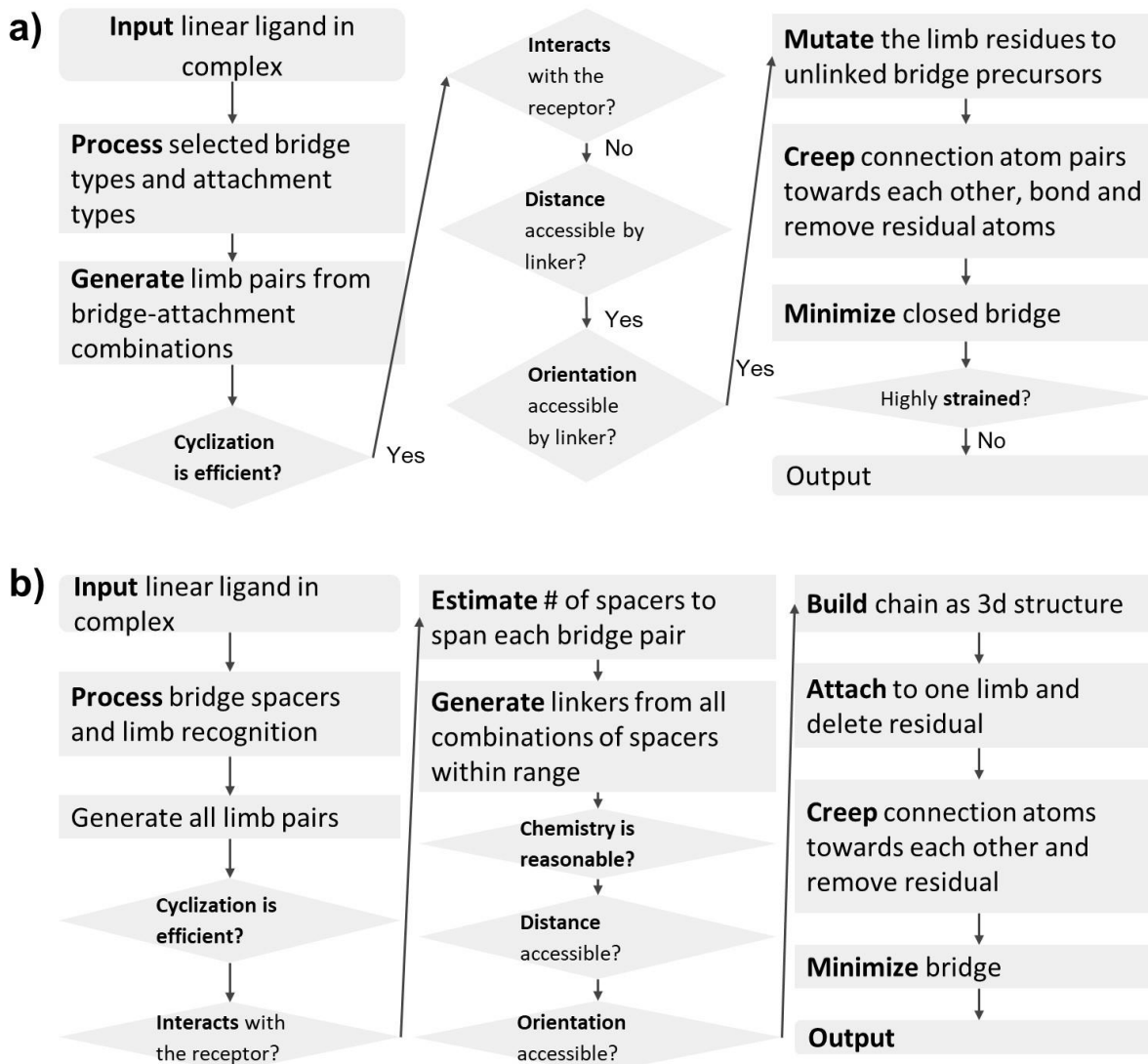
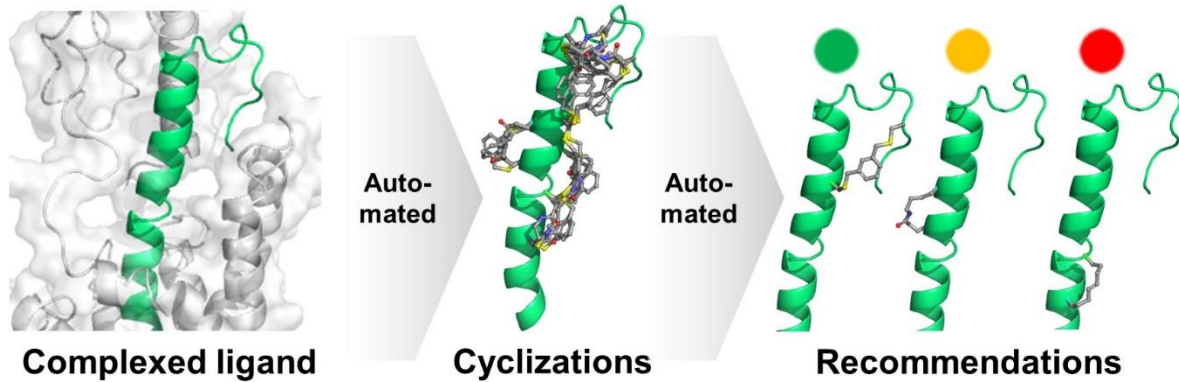


Figure 9. Workflow for a) peptides and b) small molecules.



Abstract graphic.